

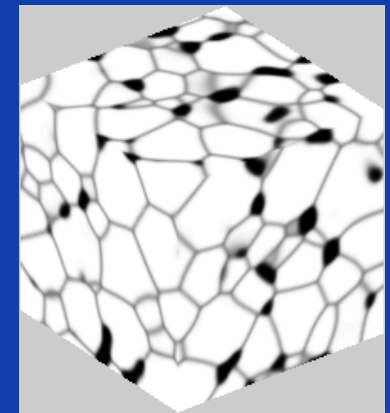
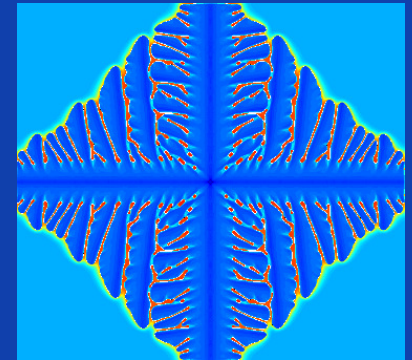
# *Quantitative phase-field modeling of growth and coarsening in polycrystalline materials*

*N. Moelans*

*Department of Metallurgy and Materials Engineering, KU Leuven, Belgium*

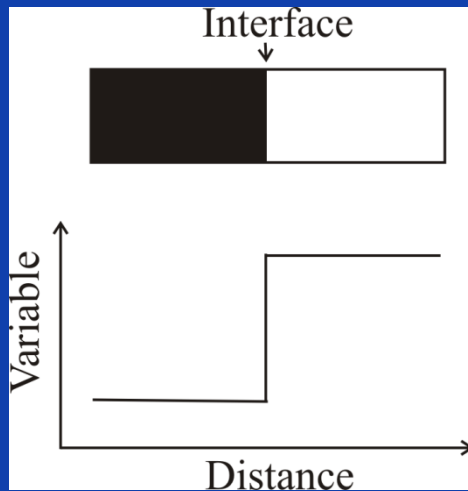
- **Some aspects of model formulation**
  - **2-phase versus multi-phase and multi-grain**
- **Application example**
  - **Slag/oxide crystallization**

- **Physics bulk and interfaces are reproduced accurately in the simulations**
  - Effect model description and parameters – Physics
  - Numerical issues
- **Predictive ?**
  - Depends on availability and accuracy of input data
    - Requires composition and orientation dependence
  - Features on the mesoscale



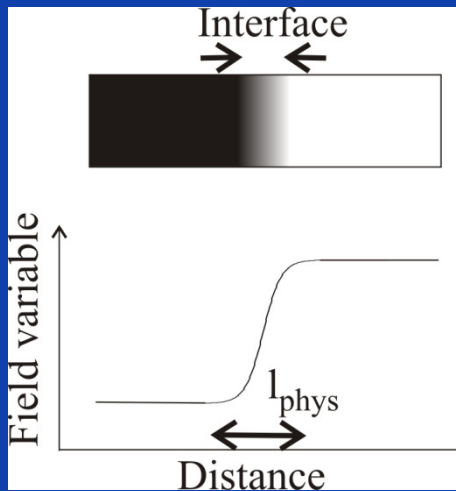
# Sharp – Diffuse – Thin interface models

## Sharp Interface



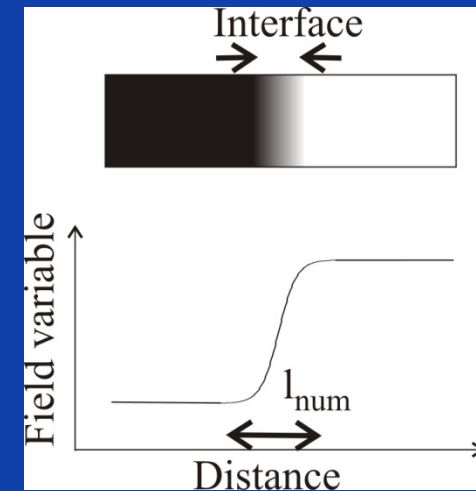
- Discontinuity
- (Semi) 1-D problems
- Problem specific

## Diffuse interface



- Complex morphologies
- Segregation, solute drag, trapping, lattice mismatch, ...
- However,  $l_{phys} (<1\text{nm}) \ll R_{grain} (\mu\text{m}-\text{mm})$
- Mostly qualitative

## Thin interface

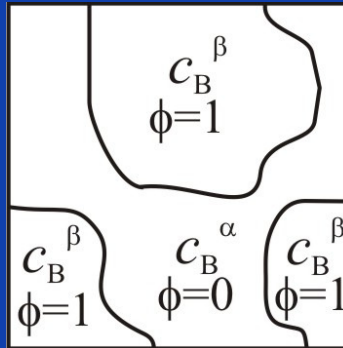
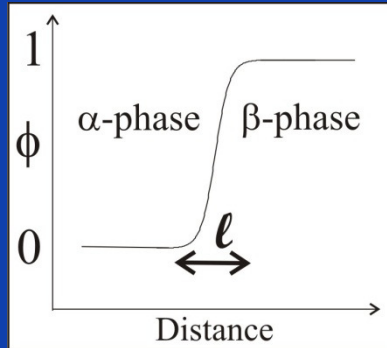


- $l_{num}$  independent
- $l_{phys} \ll l_{num} \ll R_{grain}$
- Karma and Rappel (1996), Tiaden et al. (1996), Kim and Kim (1999), Karma (2001), Kazaryan et al. (2000)

## *Some aspects of model formulation*

- **Two-phase systems : single phase-field**
- **Multi-grain/phase systems : multiple phase-field**

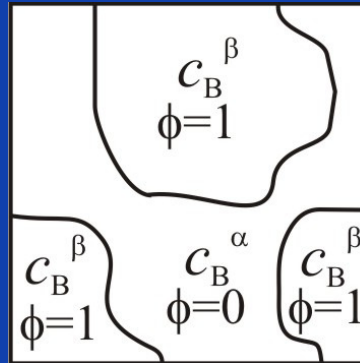
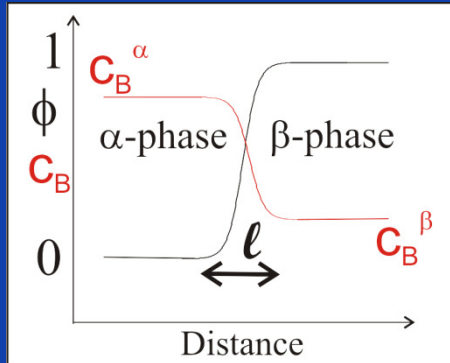
- Field variables:  $\phi(\vec{r}, t)$   $c_k(\vec{r}, t)$



- Phase  $\alpha$ :  $\phi = 0$
- Phase  $\beta$ :  $\phi = 1$
- Composition:  $c_B$

- Field variables:

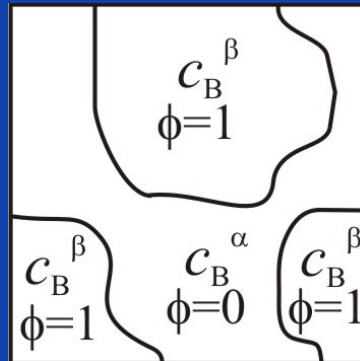
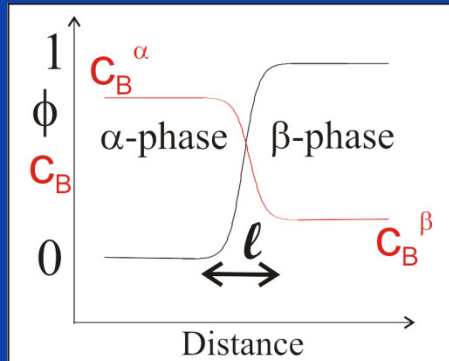
$$\phi(\vec{r}, t) \quad c_k(\vec{r}, t)$$



- Phase  $\alpha$ :  $\phi = 0$
- Phase  $\beta$ :  $\phi = 1$
- Composition:  $c_B$

- Field variables:

$$\phi(\vec{r}, t) \quad c_k(\vec{r}, t)$$

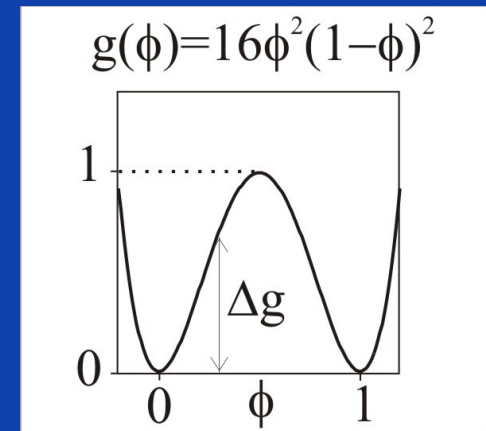


- Phase  $\alpha$ :  $\phi = 0$
- Phase  $\beta$ :  $\phi = 1$
- Composition:  $c_B$

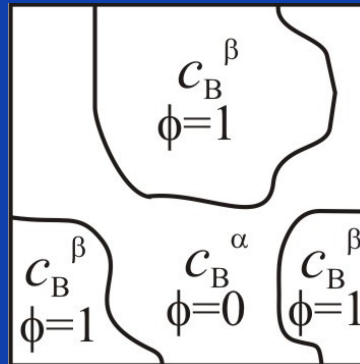
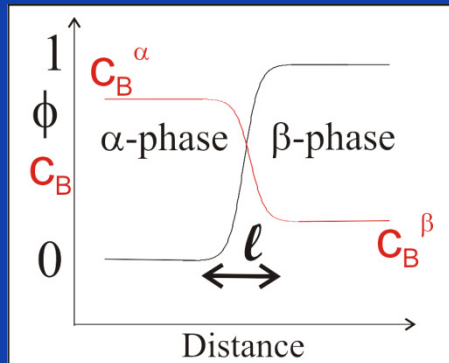
- Free energy

$$F = \int_V \left[ f_{chem}(c, \phi) + \underbrace{Wg(\phi) + \frac{\epsilon^2}{2} |\nabla \phi|^2}_{\text{Interfacial energy}} \right] d\vec{r}$$

Double well function



- Field variables:  $\phi(\vec{r}, t)$   $c_k(\vec{r}, t)$



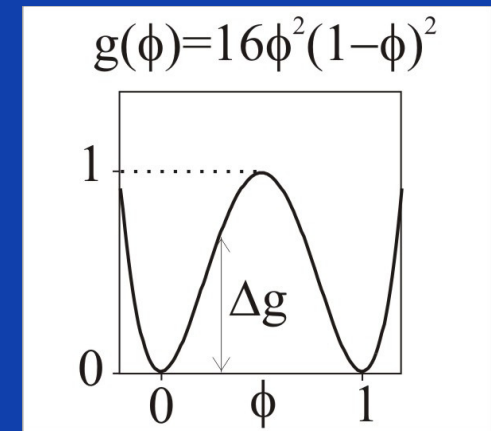
- Phase  $\alpha$ :  $\phi = 0$
- Phase  $\beta$ :  $\phi = 1$
- Composition:  $c_B$

- Free energy

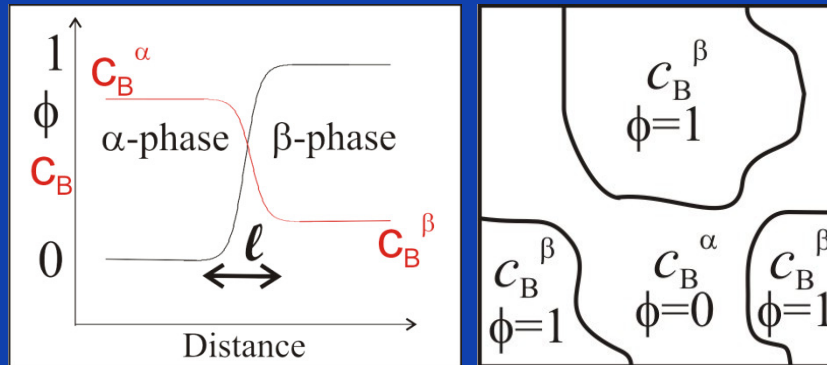
$$F = \int_V \left[ f_{chem}(c, \phi) + \underbrace{Wg(\phi) + \frac{\epsilon^2}{2} |\nabla \phi|^2}_{\text{Interfacial energy}} \right] d\vec{r}$$

$$\Rightarrow \gamma = \frac{2\sqrt{2}}{3} \sqrt{W} \epsilon, \quad l \propto \frac{\epsilon}{\sqrt{2W}}$$

Double well function



- Field variables:  $\phi(\vec{r}, t)$   $c_k(\vec{r}, t)$



- Phase  $\alpha$ :  $\phi = 0$
- Phase  $\beta$ :  $\phi = 1$
- Composition:  $c_B$

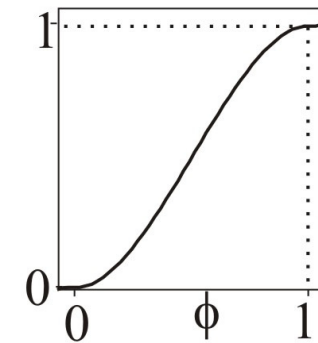
- Free energy

$$F = \int_V \left[ \underbrace{f_{chem}(c, \phi)}_{\text{Bulk energy}} + Wg(\phi) + \frac{\epsilon^2}{2} |\nabla \phi|^2 \right] d\vec{r}$$

$$f_{chem} = h(\phi) f^\beta(c, T) + [1 - h(\phi)] f^\alpha(c, T)$$

Interpolation function

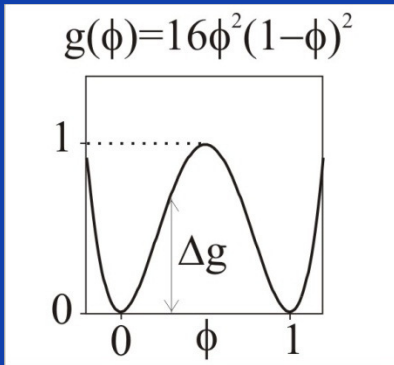
$$h(\phi) = \phi^3(10 - 15\phi + 6\phi^2)$$



- Free energy

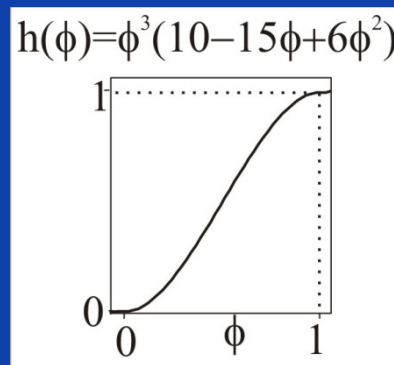
$$F = \int_V \left[ \underbrace{f_{chem}(c, \phi)}_{\text{bulk}} + Wg(\phi) + \frac{\epsilon^2}{2} |\nabla \phi|^2 \right] d\vec{r}$$

$$f_{chem} = h(\phi) f^\beta(c, T) + [1 - h(\phi)] f^\alpha(c, T)$$



Double well

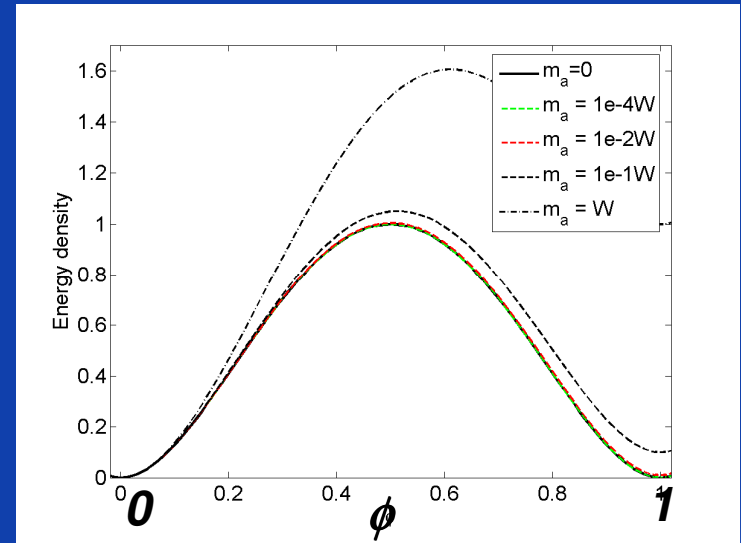
+



Bulk energy with

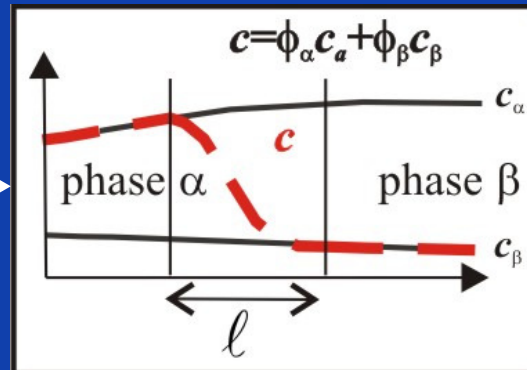
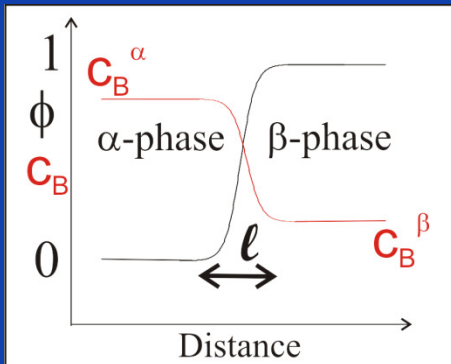
- $h(\phi)$  with zero slope at 0 and 1

=



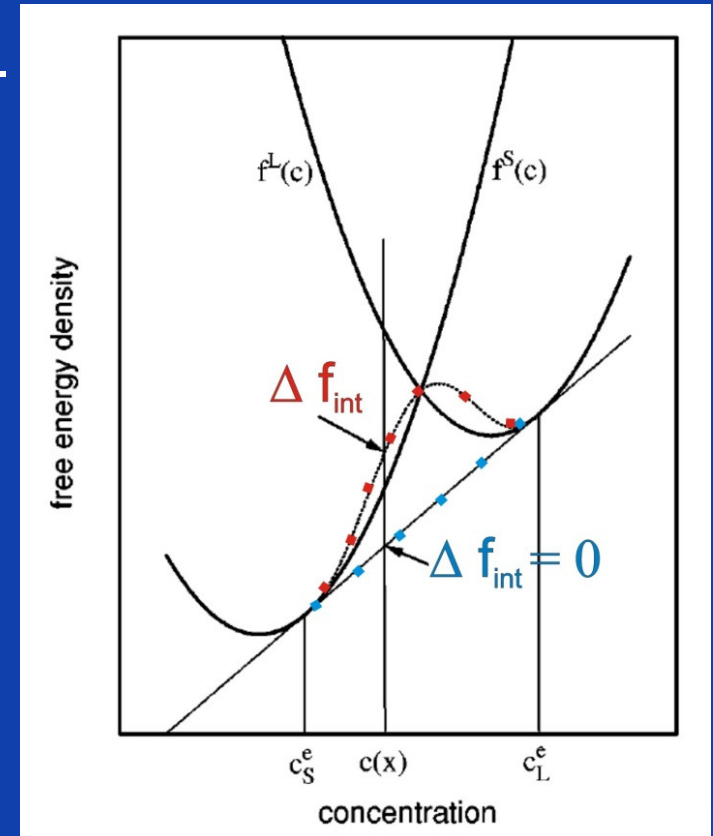
Homogeneous energy density :  
minima remain at 0 and 1

- Interface treated as mixture of 2 phases – KKS approach
  - c-field for each phase  $c \rightarrow c^\alpha, c^\beta$



- Equal diffusion or chemical potential
- Bulk energy

$$\Rightarrow f_{chem} = h(\phi) f^\beta(c^\beta) + [1 - h(\phi)] f^\alpha(c^\alpha)$$



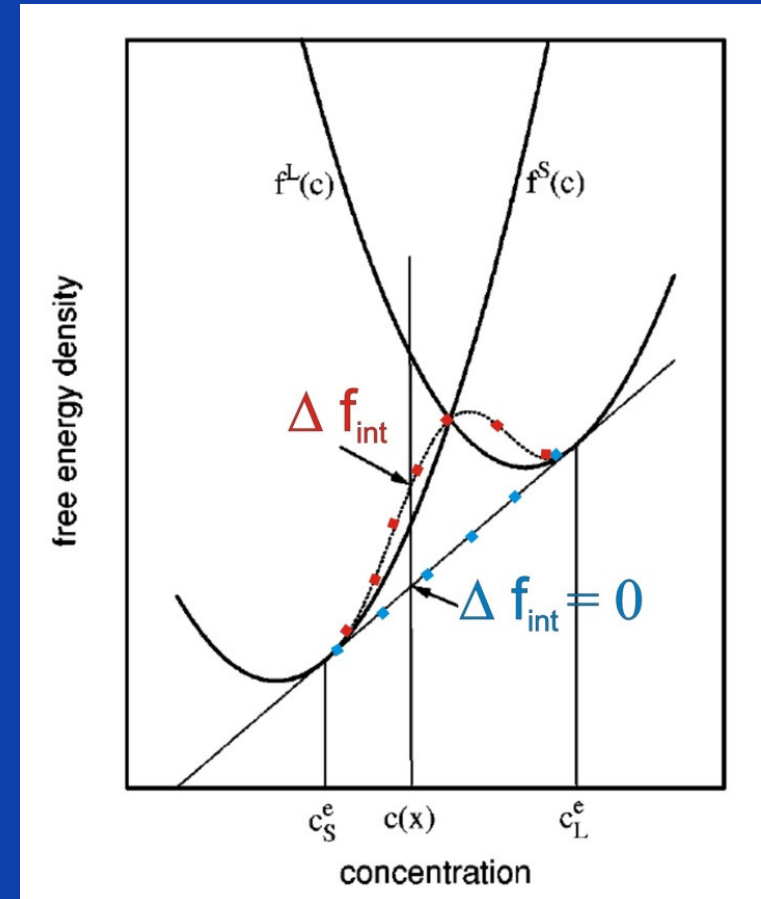
Kim et al., PRE, 6 (1999) p 7186; Tiaden et al., Physica D, 115 (1998) p73

- **Alternative formulation for dilute alloys**

*Karma 2001A. Karma, PRL, 87 (2001) n° 115701; Echebarria et al., PRE, 70 (2004) n° 061604*

- **Unified approach using a grand-canonical functional**

*M. Plapp, PRE, 84 (2011) n° 031601*



- Interface movement ( Allen - Cahn )

$$\frac{\partial \phi}{\partial t} = -L \frac{\partial F}{\partial \phi}$$

$$\frac{\partial \phi}{\partial t} = -L \left[ \underbrace{W \frac{\partial g}{\partial \phi} - \epsilon \nabla^2 \phi}_{\text{Curvature driven}} + \underbrace{\frac{\partial h}{\partial \phi} (f^\beta - f^\alpha)}_{\text{Bulk energy driven}} \right]$$

*Curvature driven    Bulk energy driven*

- Diffusion

$$\frac{\partial c_k}{\partial t} = \nabla \cdot \sum_l^{C-1} \left[ h(\phi) M_{kl}^\beta + [1 - h(\phi)] M_{kl}^\alpha \right] \nabla \tilde{\mu}_l$$

- Diffusion potentials :  $\tilde{\mu}_l = \mu_l - \mu_C$

- Diffusion mobilities/coefficients :

$$D^\rho = M^\rho G^\rho$$

$$G_{kl}^\rho = \frac{\partial^2 f^\rho}{\partial c_k \partial c_l}$$

*Multicomponent diffusion formalism of J.-O. Andersson, J. Ågren, J. Appl. Phys., J. Appl. Phys., 72 (1992) p1350*

# Decoupling bulk and interfacial kinetics

- Anomalous nonequilibrium effects, such as discontinuity in  $\mu_i$  for  $D_i \neq D_s$

$$\propto \ell, v_n, \vec{j}_n$$

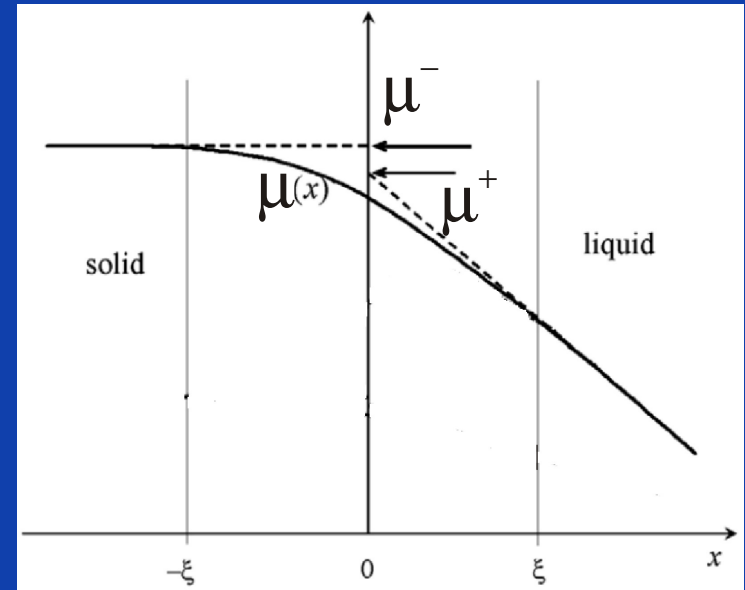
- Non-variational anti-trapping current

$$\vec{j}_a = \alpha \sqrt{\frac{\kappa}{W}} \left( 1 - \frac{D_s}{D_L} \right) \frac{\partial \phi}{\partial t} \frac{\nabla \phi}{|\nabla \phi|}$$

- But still ‘Kapitza’ effect for

$$\vec{j}_n \gg v_n$$

M. Plapp, *Phil. Mat.* 91 (2011) p25



- Anomalous effects: R.F. Almgren, *SIAM J. Appl. Math.*, 59 (1999) p2086.
- Anti-trapping, dilute,  $D_S=0$ : A.Karma, *PRL*, 87, 115701 (2001); B. Echebarria et al., *PRE*, 70, 061604 (2004)
- Anti-trapping, dilute,  $D \neq 0$ : M. Ohno and K. Matsuura, *Phys. Rev. E* 79 (2009) No 031603
- Anti-trapping multi-comp,  $D_S=0$ : S.G. Kim, *Acta Mater.* 55, p4391 (2007)

## *Some aspects of model formulation*

- Two-phase systems : single phase-field
- **Multi-grain/phase systems : multiple phase-field**

- Single phase-field models -> Multiple phase-field models

$$\phi \rightarrow \{\phi_1, \phi_2, \phi_3, \dots, \phi_p\}$$

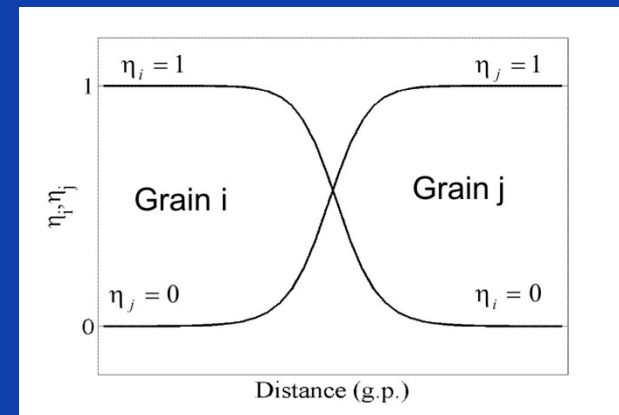
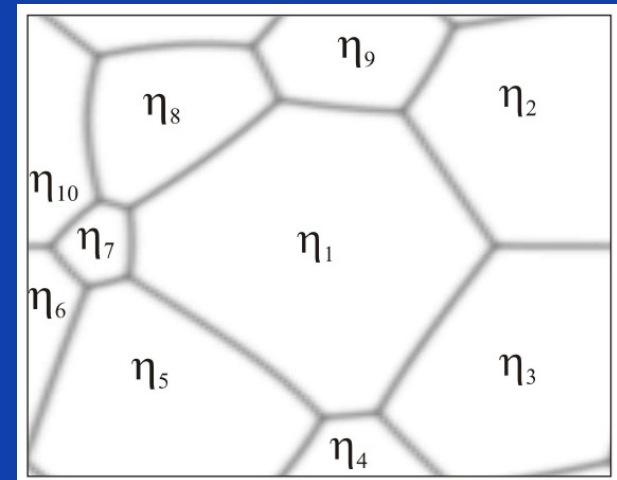
- Model extension

$$F(\phi_1, \phi_2, \phi_3, \dots, |\nabla \phi_1|^2, |\nabla \phi_2|^2, \dots)$$

- Different types of interfaces
- Triple and higher order junctions

- Numerically

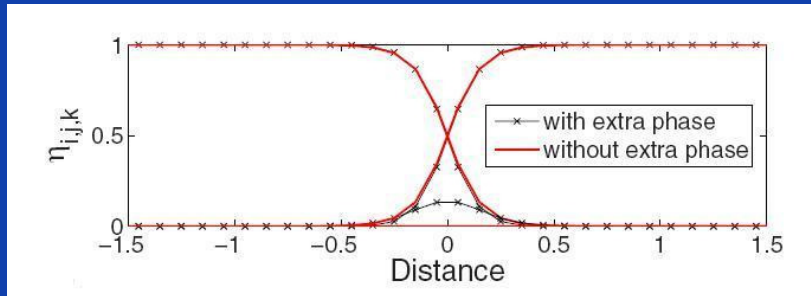
- Homogeneous accuracy
- Thin interface asymptotics for all interfaces  $\rightarrow \ell_{num} = cte$



# Multi-grain and multi-phase models: major difficulties

- **Third-phase contributions**

- $\sigma_{12} = \sigma_{13} = 7/10 \sigma_{12}$



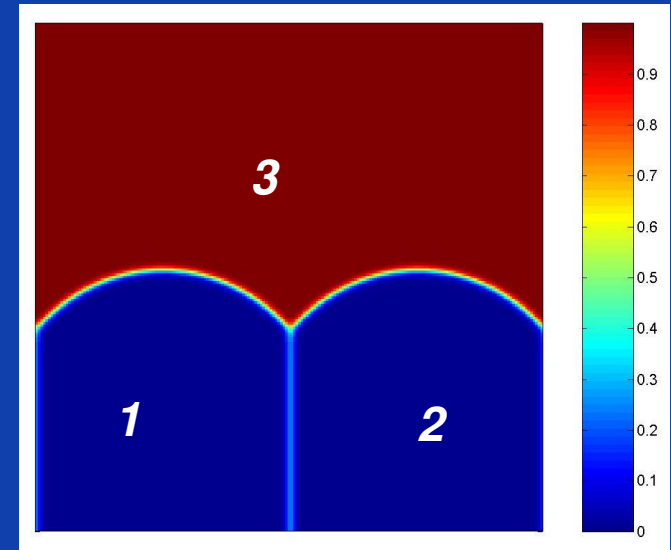
- → Careful choice of multi-well function and gradient contribution

- **Interpolation function**

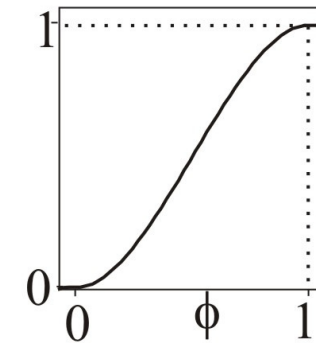
- Zero-slope at equilibrium values of the phase fields
  - Thermodynamic consistency

$$f_{chem} = \sum_{i=1}^p h_i(\eta_1, \eta_2, \dots) f^i(c, T) \Rightarrow \sum_{i=1}^p h_i(\eta_1, \eta_2, \dots) = 1$$

$\eta_3$



$$h(\phi) = \phi^3(10 - 15\phi + 6\phi^2)$$



## *Some aspects of model formulation*

- Two-phase/grain model
- **Multi-grain model**
- Multi-phase multi-grain model

- **Phase fields**  $\eta_1, \eta_2, \dots, \eta_i(\vec{r}, t), \dots, \eta_p$ 
  - **With grain i**  
 $(\eta_1, \eta_2, \dots, \eta_i, \dots, \eta_p) = (0, 0, \dots, 1, \dots, 0)$

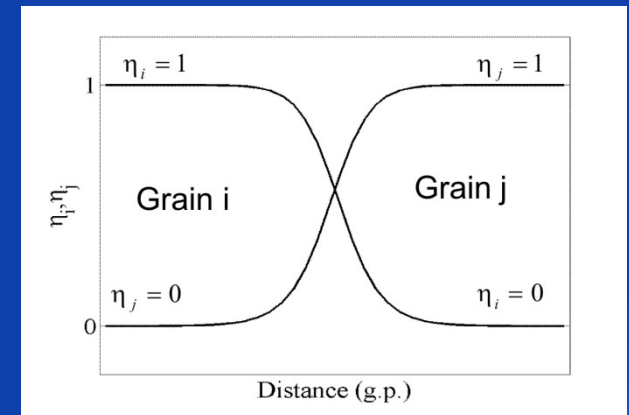
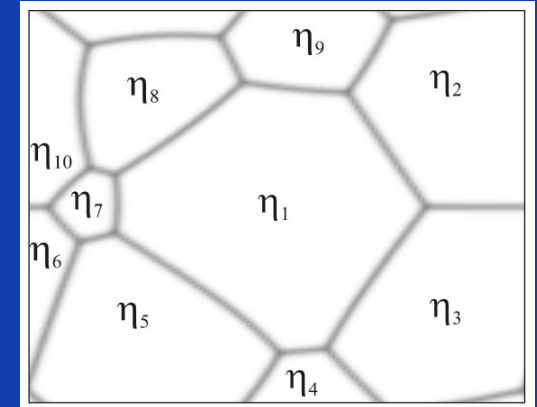
- **Free energy**

$$F_{interf} = \int_V m \left( \sum_{i=1}^p \left( \frac{\eta_i^4}{4} - \frac{\eta_i^2}{2} \right) + \sum_{i=1}^p \sum_{j<i}^p \gamma_{i,j} \eta_i^2 \eta_j^2 + \frac{1}{4} \right) + \frac{\kappa(\eta)}{2} \sum_{i=1}^p (\nabla \eta_i)^2 dV$$

$$\kappa(\eta) = \frac{\sum_{i=1}^p \sum_{j<i}^p \kappa_{i,j} \eta_i^2 \eta_j^2}{\sum_{i=1}^p \sum_{j<i}^p \eta_i^2 \eta_j^2}$$

- **For each grain boundary**  $\eta_i^2 \eta_j^2 \neq 0 \Rightarrow \kappa(\eta) = \kappa_{i,j}$
- **Inclination dependence**

$$\gamma_{i,j}(\psi_{i,j}), \kappa_{i,j}(\psi_{i,j}), L_{i,j}(\psi_{i,j}), \quad \psi_{i,j} = \frac{\nabla \eta_i - \nabla \eta_j}{|\nabla \eta_i - \nabla \eta_j|}$$



A. Kazaryan et al., PRB, 61 (2000) p14275

# Non-variational approach – equal interface width

- Ginzburg-Landau type equations

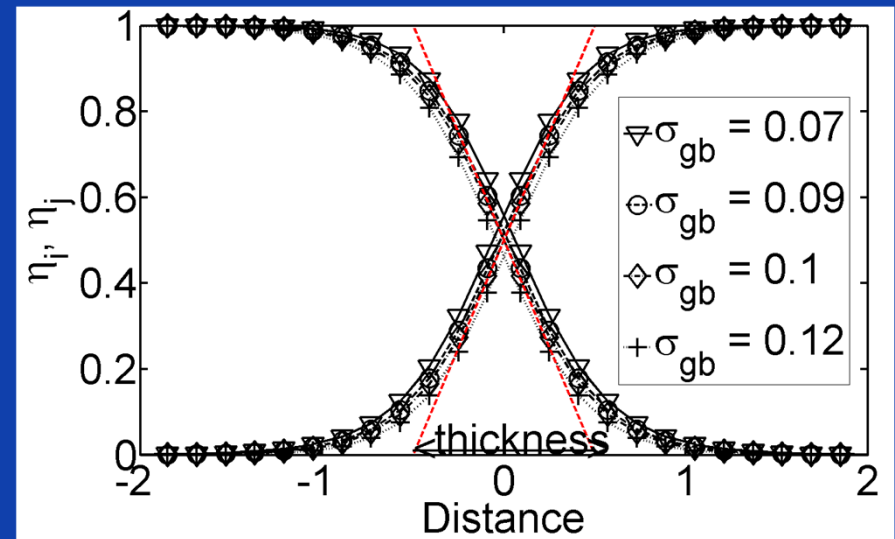
$$\frac{\partial \eta_i(\vec{r}, t)}{\partial t} = -L(\eta) \left[ m \left( \eta_i^3 - \eta_i + 2\eta_i \sum_{j \neq i} \gamma_{i,j} \eta_j^2 \right) - \kappa(\eta) \nabla^2 \eta_i \right]$$

- Non-variational with respect to  $\eta$ -dependence of  $\kappa$
- Similar to Monte Carlo Potts approach

- Definition ‘grain boundary width’

$$l_{num} = \frac{1}{\left| \frac{d\eta_i}{dx} \right|_{max}} = \frac{1}{\left| \frac{d\eta_j}{dx} \right|_{max}}$$

→ High controllability of numerical accuracy ( $l_{num}/R < 5$ )



- Grain boundary energy

$$\gamma_{gb,\theta_{i,j}} = g(\gamma_{i,j}) \sqrt{m \kappa_{i,j}}$$

- Grain boundary mobility

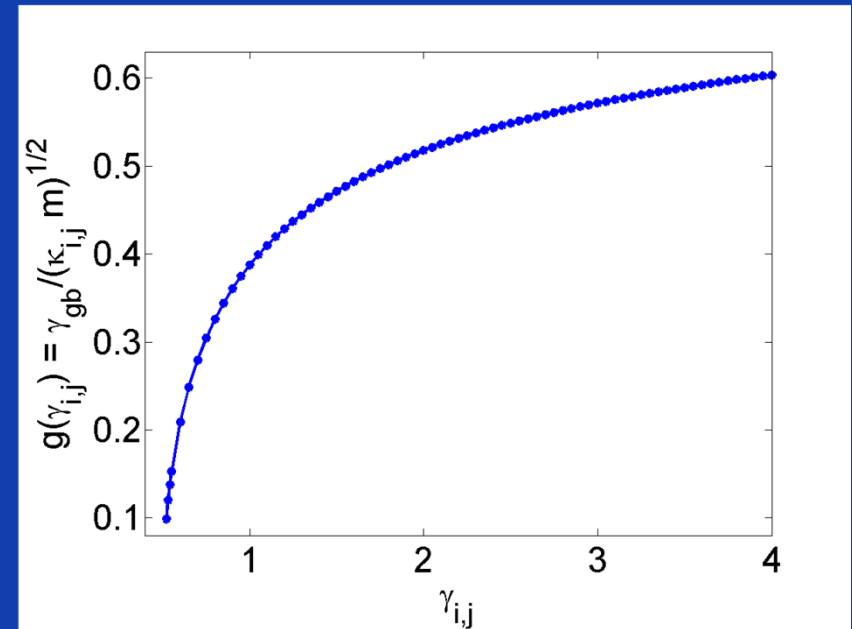
$$\mu_{gb,\theta_{i,j}} = L_{i,j} \sqrt{\frac{\kappa_{i,j}}{m(g(\gamma_{i,j}))^2}}$$

- Grain boundary width

$$l = \frac{4}{3} \sqrt{\frac{\kappa_{i,j}}{m(g(\gamma_{i,j}))^2}}$$

- Iterative algorithm

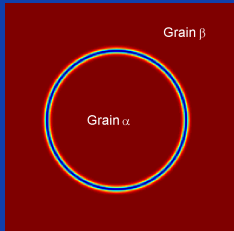
$$l_{gb}, [\gamma_{gb,\theta}], [\mu_{gb,\theta}] \rightarrow m, [\kappa_{i,j}], [\gamma_{i,j}], [L_{i,j}]$$



*g(γ<sub>i,j</sub>) calculated numerically*

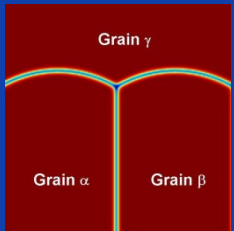
N. Moelans, B. Blanpain, P. Wollants,  
*PRL*, 101, 0025502 (2008); *PRB*, 78,  
024113 (2008)

- Shrinking grain:



$$\frac{dA_\alpha}{dt} = -2\pi\mu_{\alpha\beta}\sigma_{\alpha\beta}$$

- Triple junction angles:

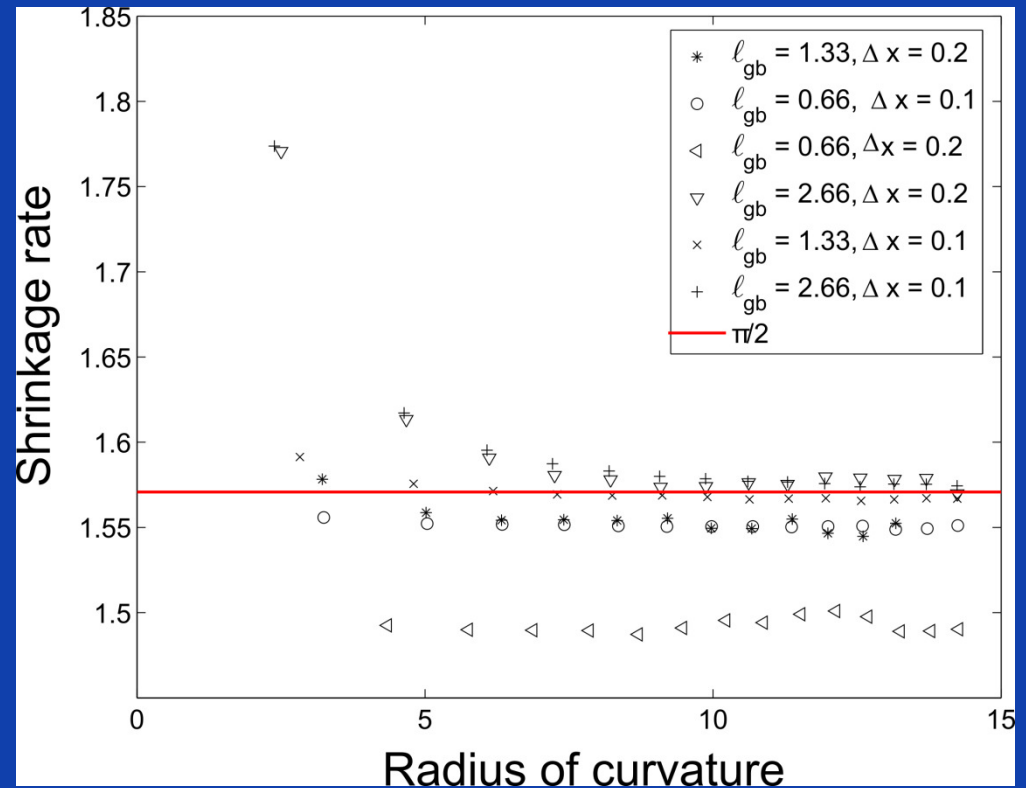


$$\frac{dA_\alpha}{dt} = -\mu_{\alpha\gamma}\sigma_{\alpha\beta}$$

$$\sigma_{\alpha\gamma} = \sigma_{\beta\gamma}, \mu_{\alpha\gamma} = \mu_{\beta\gamma}$$

- Observations

- Accuracy controlled by  $l_{num} / \Delta x$  for  $l_{num} / R \leq 5$
- Diffuse interface effects for  $l_{num} / R \geq 5$
- Angles outside [100°-140°] require larger  $l_{num} / \Delta x$  for same accuracy



# Variational approach – interface width varies with interface energy

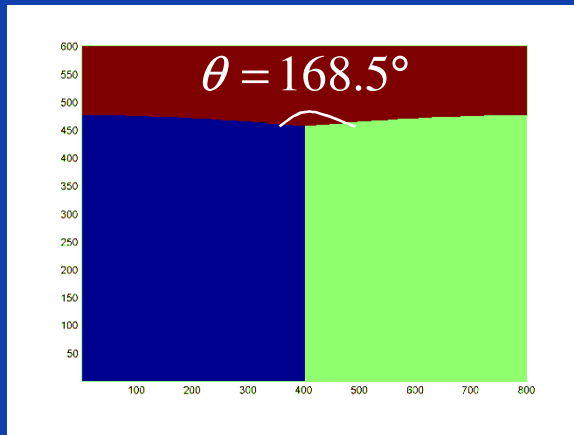
- Anisotropy only through  $\gamma_{i,j}$   $\kappa=cte$

- Energy

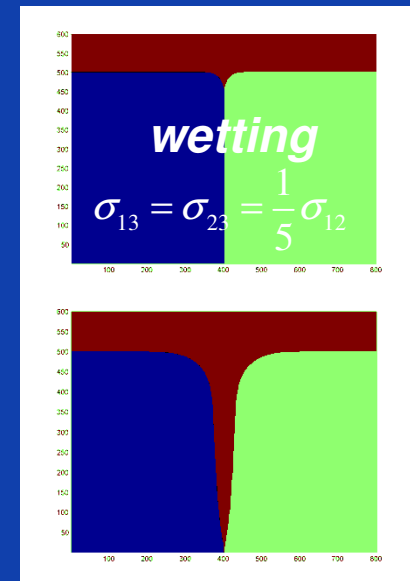
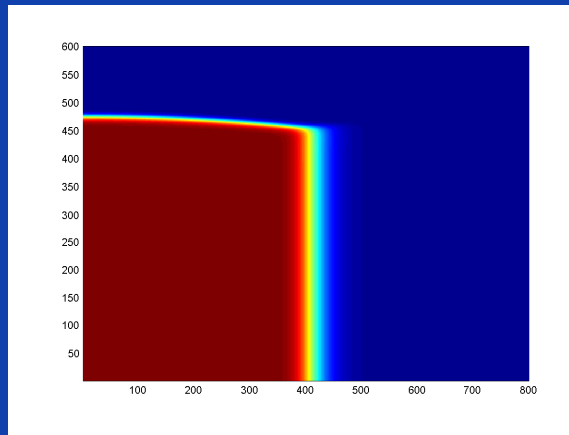
$$F = \int_V \left[ m \left( \sum_{i=1}^p \left( \frac{\eta_i^4}{4} - \frac{\eta_i^2}{2} \right) + \sum_{i=1}^p \sum_{j<i}^p \gamma_{i,j} \eta_i^2 \eta_j^2 + \frac{1}{4} \right) + \frac{\kappa}{2} \sum_{i=1}^p (\vec{\nabla} \eta_i)^2 \right] dV$$

- Kinetic equations

$$\frac{\partial \eta_i(\vec{r}, t)}{\partial t} = -L(\eta) \left[ m \left( \eta_i^3 - \eta_i + 2\eta_i \sum_{j \neq i} \gamma_{i,j} \eta_j^2 \right) - \kappa \nabla^2 \eta_i \right]$$



$$\sigma_{13} = \sigma_{23} = 5\sigma_{12}$$



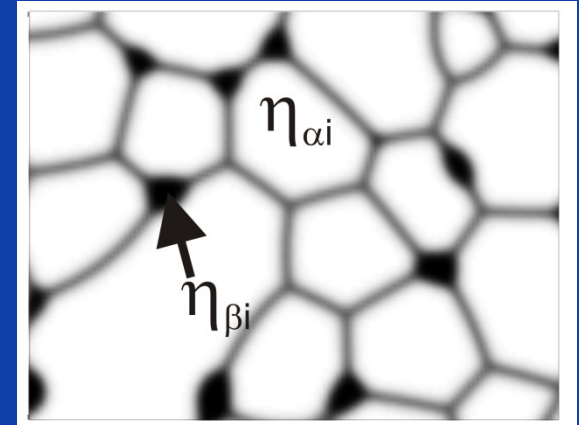
## *Some aspects of model formulation*

- Two-phase/grain model
- Multi-grain model
- **Multi-phase multi-grain model**

# Extension to multi-component multi-phase alloys

- Phase field variables:

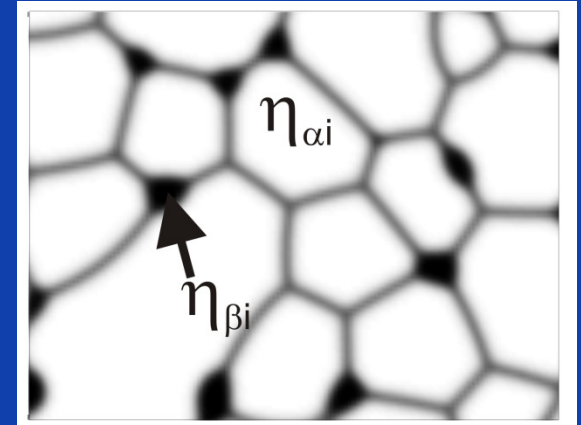
- Grains  $\eta_{\alpha_1}, \eta_{\alpha_2}, \dots, \eta_{\alpha_i}(\vec{r}, t), \dots,$   
 $\eta_{\beta_1}, \eta_{\beta_2}, \dots, \eta_p$
- Composition  $x_A, x_B(\vec{r}, t), \dots, x_{C-1}$



# Extension to multi-component multi-phase alloys

- Phase field variables:

- Grains  $\eta_{\alpha 1}, \eta_{\alpha 2}, \dots, \eta_{\alpha i}(\vec{r}, t), \dots,$
- Composition  $\eta_{\beta 1}, \eta_{\beta 2}, \dots, \eta_{\beta p}$
- Composition  $x_A, x_B(\vec{r}, t), \dots, x_{C-1}$



- Bulk energy:  $f_{bulk}(x_k, \eta_{\rho i}) = \sum_{\rho} \phi_{\rho} f^{\rho}(x_k^{\rho})$

- with

$$\left\{ \begin{array}{l} \frac{\partial f^{\beta}(x_k^{\beta})}{\partial x_k^{\beta}} = \frac{\partial f^{\alpha}(x_k^{\alpha})}{\partial x_k^{\alpha}} = \dots = \tilde{\mu}_k \\ x_k = \sum_{\rho} \phi_{\rho} x_k^{\rho} \end{array} \right. \quad \text{and} \quad \phi_{\rho} = \frac{\sum_i \eta_{\rho i}^2}{\sum_{\pi=\alpha, \beta, \dots} \sum_i \eta_{\pi i}^2}$$

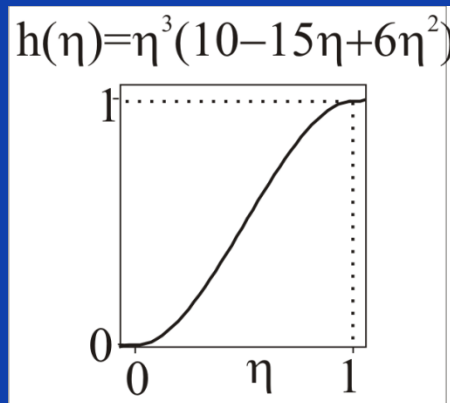
**KKS approach**

**Interpolation function**

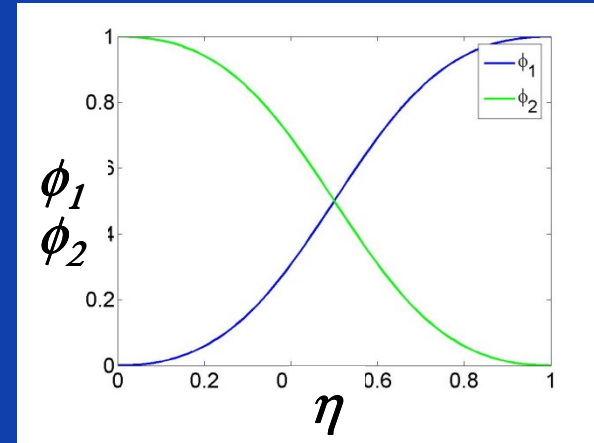
- Bulk energy:**  $f_{bulk}(x_k, \eta_{\rho i}) = \sum_{\rho} h_{\rho}(\eta_{\rho i}) f^{\rho}(x_k^{\rho})$

- With  $h_{\rho}(\eta_{\rho i}) = \phi_{\rho} = \frac{\sum_i \eta_{\rho i}^2}{\sum_{\pi=\alpha, \beta, \dots} \sum_i \eta_{\pi i}^2}$  and  $f^{\rho}(x_k^{\rho}) = \frac{G_m^{\rho}(x_k^{\rho})}{V_m}$

Replaces the standard function for 2-phase systems



Interpolation function for 2-phase system



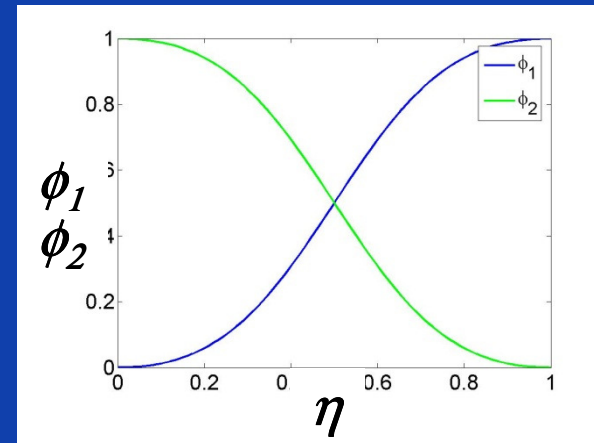
Interpolation functions for multi-phase system

N. Moelans, *Acta Mater*, 59, 1077-1086, 2011

- Interpolation function

$$h_\rho(\eta_{\rho i}) = \phi_\rho = \frac{\sum_i \eta_{\rho i}^2}{\sum_{\pi=\alpha,\beta,\dots} \sum_i \eta_{\pi i}^2}$$

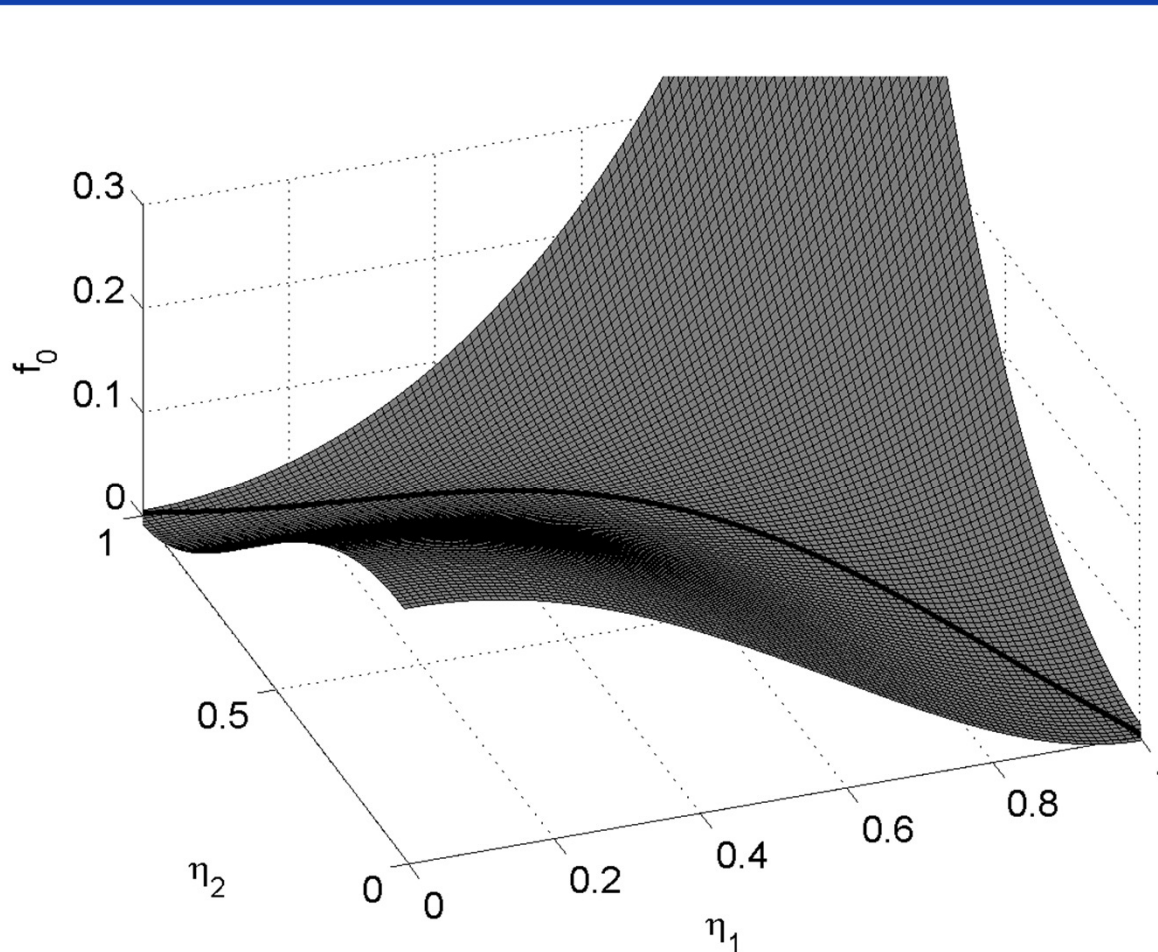
$$\left\{ \begin{array}{l} \sum_\rho \phi_\rho = 1 \Rightarrow \text{'phase fractions'} \\ \frac{\partial \phi_\rho}{\partial \eta} \Big|_{\eta=0, \eta=1} = 0 \Rightarrow \text{Minima remain at} \\ \qquad \qquad \qquad (0, 0, \dots, 1, \dots, 0) \end{array} \right.$$



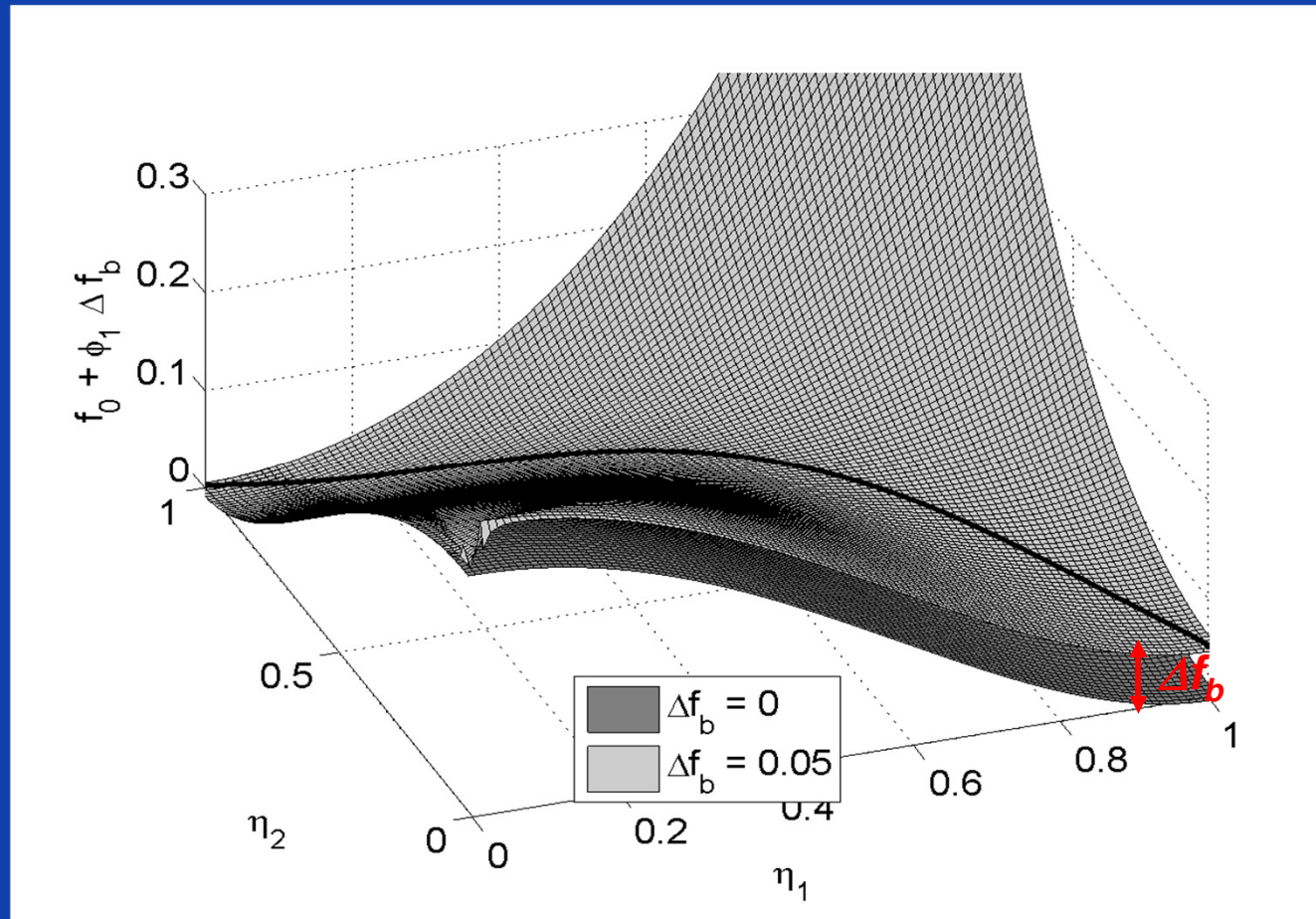
Interpolation functions for multi-phase system

N. Moelans, *Acta Mater*, 59, 1077-1086, 2011

- Only Interfacial energy :  $f = f_0(\eta_\alpha, \eta_\beta)$



- Interfacial + bulk energy :  $f = f_0(\eta_\alpha, \eta_\beta) + \phi_\alpha f^\alpha + \phi_\beta f^\beta$



# Equations for interface movement

- Interface movement: 
$$\frac{\partial \eta_{i\rho}}{\partial t} = -L \frac{\delta F(\eta_{i\rho}, x_k)}{\delta \eta_{i\rho}}$$

- Grain boundary between grain  $\rho,i$  and  $\rho,j$

$$\frac{\partial \eta_{\rho i}}{\partial t} = -L \left( \frac{\partial f_{interf}}{\partial \eta_{\rho i}} - \kappa_{i,j} \nabla^2 \eta_{\rho i} \right) = -L g_{int}(\eta, \nabla \eta)$$

- Between phase  $\alpha$  and  $\beta$

$$\frac{\partial \eta_{\alpha i}}{\partial t} = -L \left( g_{int}(\eta, \nabla \eta) + \frac{v \eta_{\alpha i}^{v-1} \eta_{\beta j}^v}{(\eta_{\alpha}^v + \eta_{\beta}^v)^2} (f^{\alpha}(x^{\alpha}) - f^{\beta}(x^{\beta}) - (x^{\alpha} - x^{\beta}) \tilde{\mu}) \right)$$

Curvature driven

Bulk energy driven

- Diffusion flux (of the form  $\vec{J}_k = -\sum_{l=1}^{C-1} M_{kl} \nabla(\mu_l - \mu_C) = -\sum_{l=1}^{C-1} M_{kl} \nabla \tilde{\mu}_l$ )

J.-O. Andersson, J. Ågren, J. Appl. Phys., J. Appl. Phys., 72 (1992) p1350

- E.g. for binary A-B

$$\vec{J}_B = \frac{-1}{V_m} \left( \sum_{\rho} \phi_{\rho} M^{\rho} + \sum_{\rho, i \neq \sigma, j} M_{interf} \eta_{\rho, i}^2 \eta_{\sigma, j}^2 \right) \nabla \tilde{\mu}_B$$

*Bulk diffusion*

*Interface diffusion*

- Relation with interdiffusivities

$$M^{\rho} = D^{\rho} \left/ \frac{\partial^2 f^{\rho}}{\partial x_B^2} \right.$$

- Relation with atomic mobilities

$$M^{\rho} = x_B (1 - x_B) (x_B \beta_A^{\rho} + (1 - x_A) \beta_B^{\rho})$$

- Relation with pipe interdiffusivities

$$M_{interf} = 3 \left( \frac{D_{interf}}{\partial^2 f^m / \partial x_B^2} \right) \left( \frac{\delta_{gb}}{\delta_{num}} \right)$$

- Mass conservation

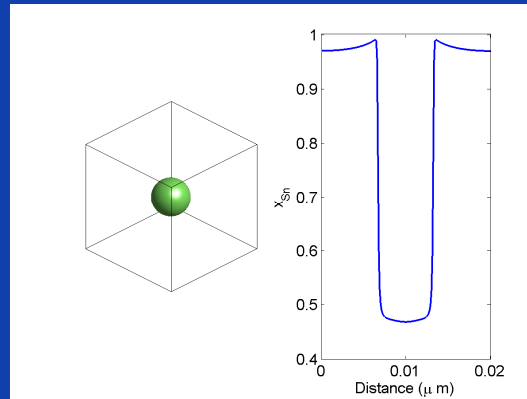
$$\frac{\partial x_B}{\partial t} = \nabla \cdot \left[ \left( \sum_{\rho} \phi_{\rho} M^{\rho} + \sum_{\rho, i \neq \sigma, j} M_s \eta_{\rho, i}^2 \eta_{\sigma, j}^2 \right) \nabla \tilde{\mu}_B \right]$$

# Effect of diffuse interface width: Numerical validation

- **Triple junction**



- **Growing sphere**



- **Processes for which**

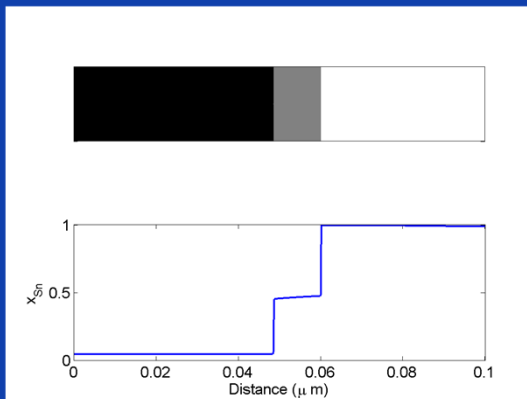
$v(t) \searrow$

- **Accuracy controlled by  $\ell_{num} / \Delta x$**   
( $\approx 1.3\%$  for 6 g.p.,  $< 1\%$  for 10 g.p.)

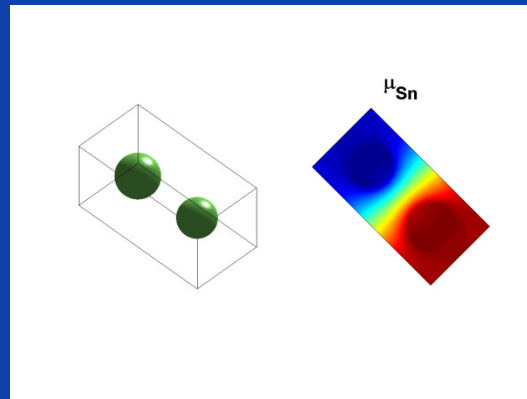
- **Diffuse interface effects for  $\ell_{num} / R > 5$**

- **Angles outside  $[100^\circ - 140^\circ]$  require larger resolution for same accuracy**

- **Intermediate phase**



- **Coarsening**



*N. Moelans, Acta Mater, 59, 1077-1086, 2011*

- **Multi-phase-field model**

- **Phase fields**  $\phi_1, \phi_2, \phi_3, \dots, \phi_p, \sum_{i=1}^p \phi_i = 1$

- **Interfacial energy**  $f_{\text{int}} = \sum_{i \neq j} \frac{4\sigma_{i,j}}{\eta_{i,j}} \left\{ \frac{\eta_{i,j}^2}{\pi^2} |\nabla \phi_i \cdot \nabla \phi_j| + \phi_i \phi_j \right\} + \sum_{i \neq j} \sum_{k \neq i,j} W_{ijk} \phi_i \phi_j \phi_k$   
 $0 < \phi_{i,j} < 1$

- **Multi-order parameter models**

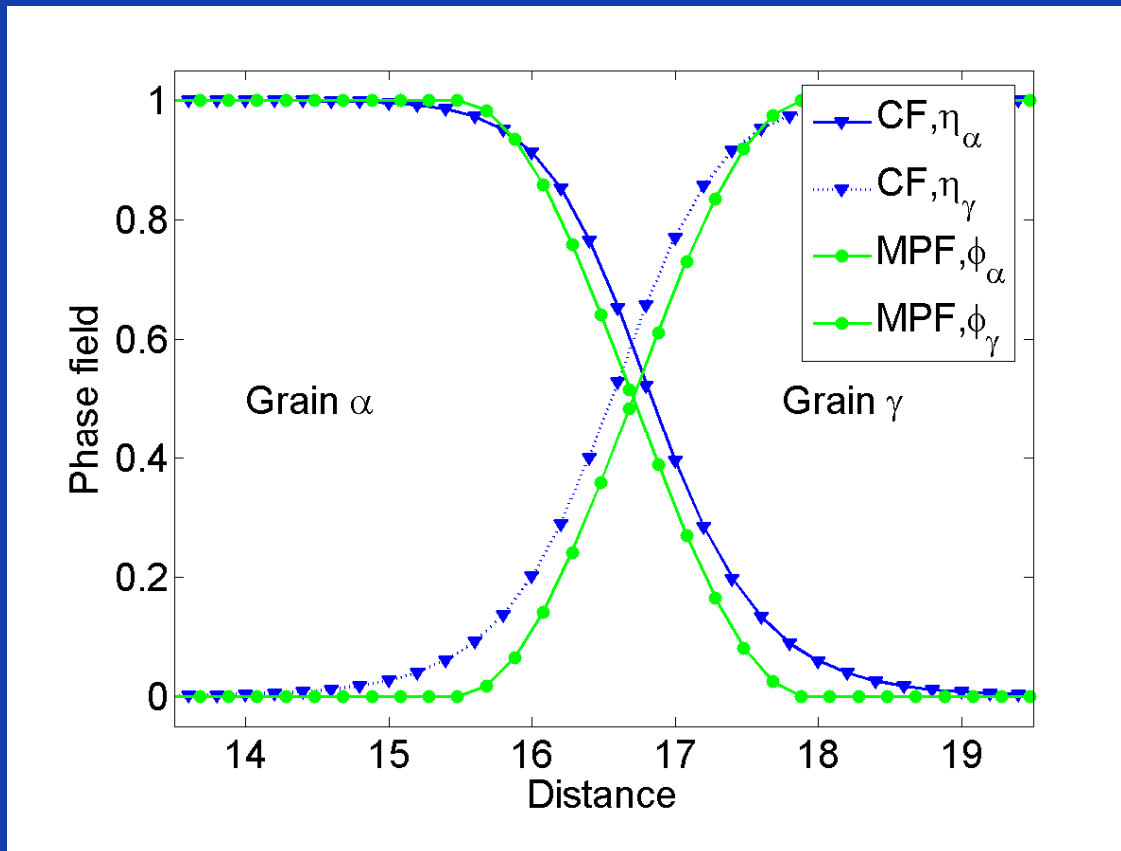
- **Order parameters**  $\eta_1, \eta_2, \dots, \eta_i(\vec{r}, t), \dots, \eta_p, \left( \sum_{i=1}^p \eta_i \neq 1 \right)$

- **Interfacial energy**  $f_{\text{int}} = m \left( \sum_{i=1}^p \left( \frac{\eta_i^4}{4} - \frac{\eta_i^2}{2} \right) + \sum_{i=1}^p \sum_{j < i} \gamma_{i,j} \eta_i^2 \eta_j^2 + \frac{1}{4} \right) + \frac{\kappa(\eta)}{2} \sum_{i=1}^p (\vec{\nabla} \eta_i)^2$   
 $\kappa(\eta) = \frac{\sum_{i=1}^p \sum_{j < i} \kappa_{i,j} \eta_i^2 \eta_j^2}{\sum_{i=1}^p \sum_{j < i} \eta_i^2 \eta_j^2}$

*N. Moelans, F. Wendler, B. Nestler, Comp. Mater. Sci. 46 (2009) p479*

# Model comparison : individual interface

- For 'equivalent' model parameters



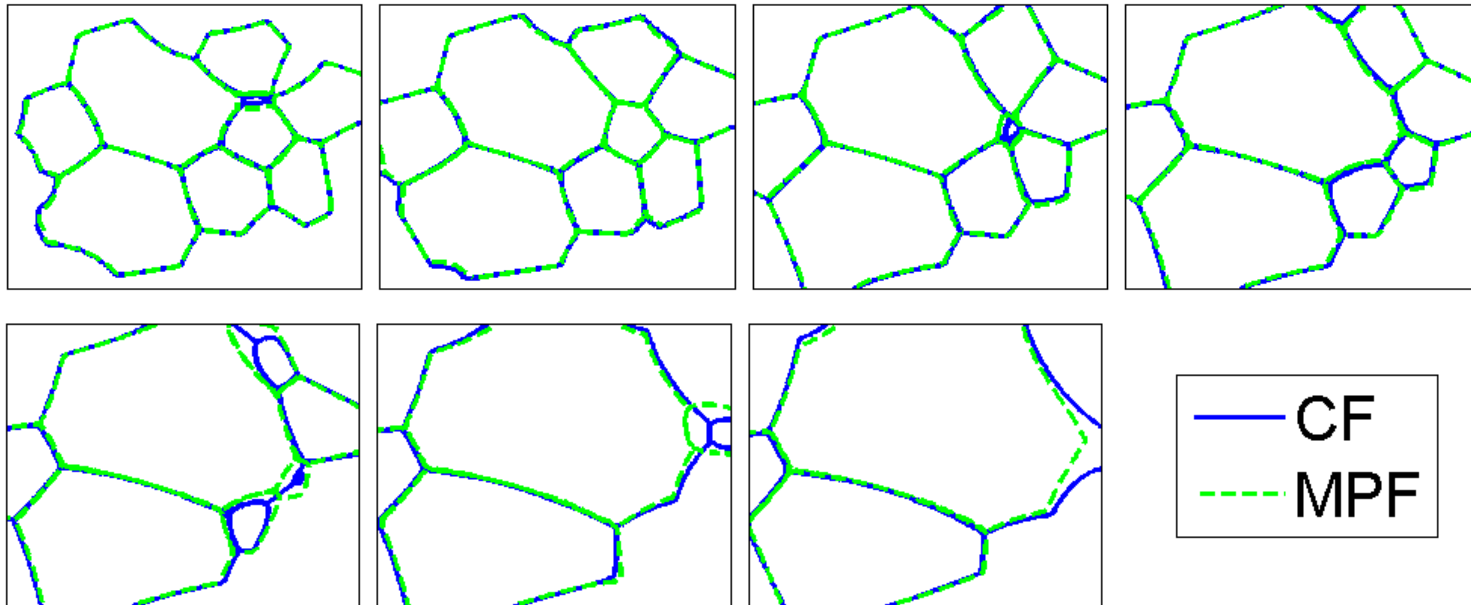
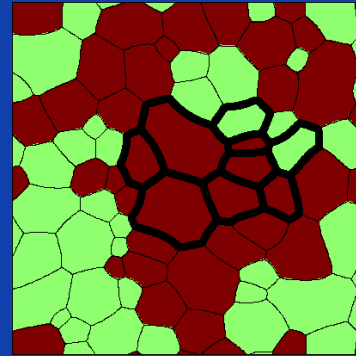
- Similar accuracy for 2- and 3-grain structures for grain boundary movement

- Choice  $W_{ijk}$  in MPF affects triple-junction angles

- MPF can reproduce very low and high angles more accurate than the non-variational CF

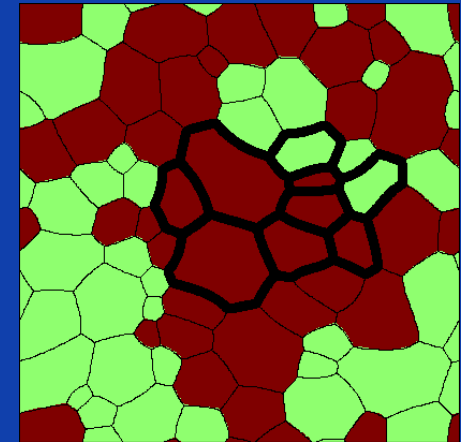
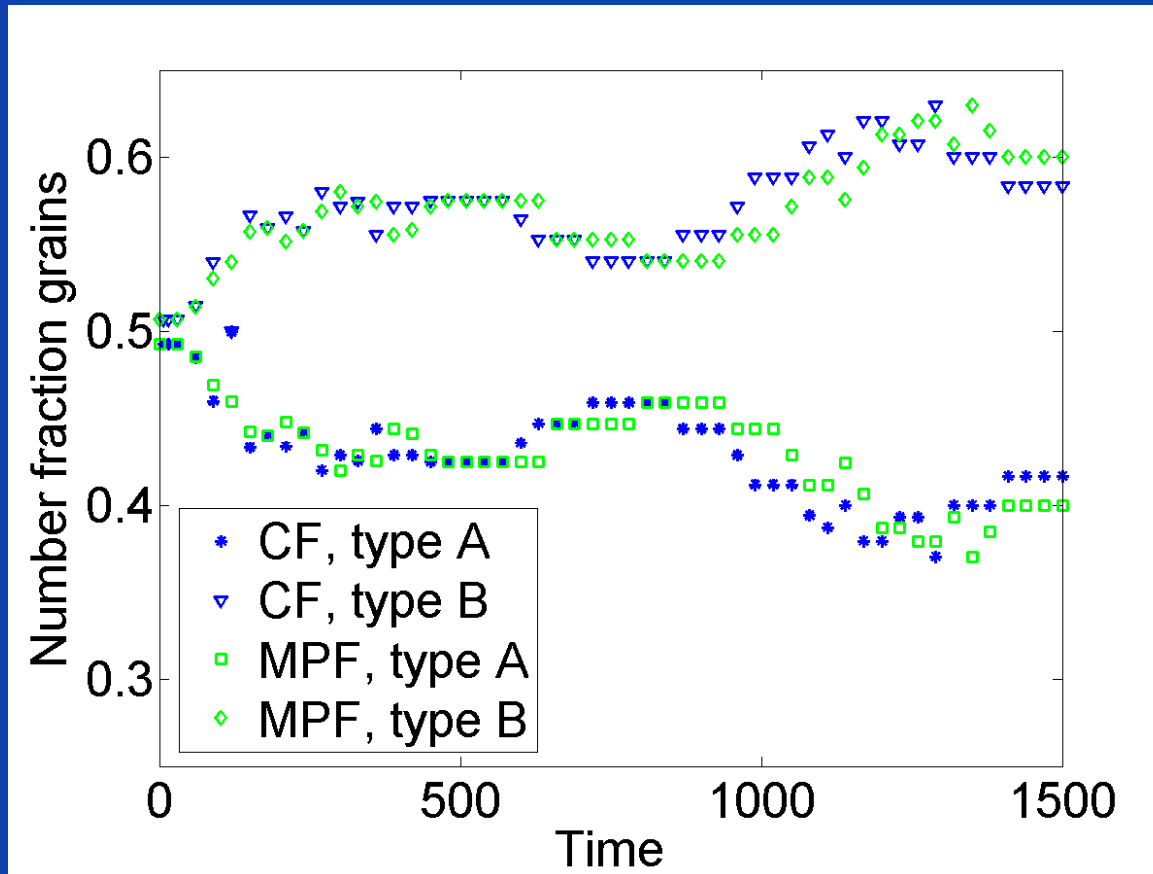
N. Moelans, F. Wendler, B. Nestler, *Comp. Mater. Sci.* 46 (2009) p479

- 2 orientation variants

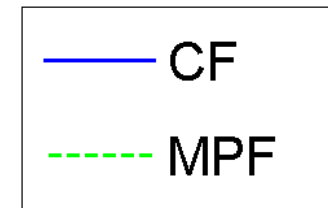
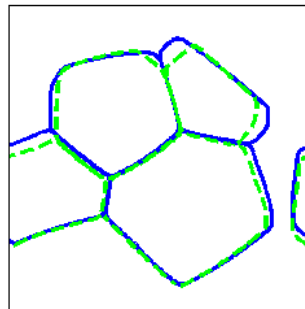
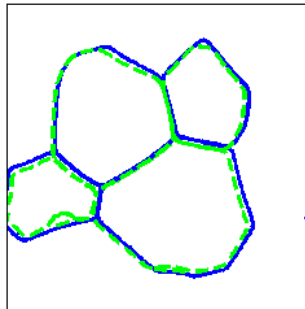
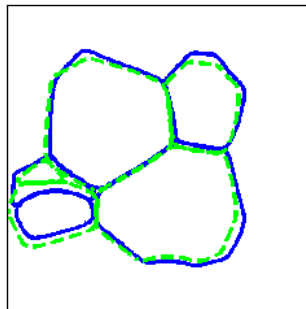
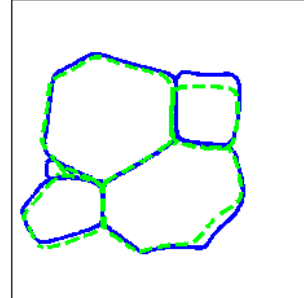
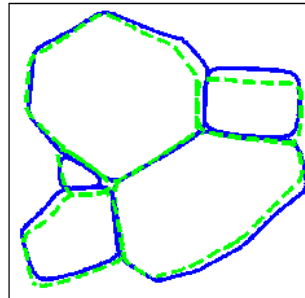
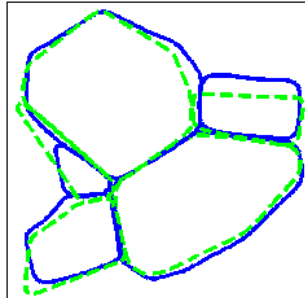
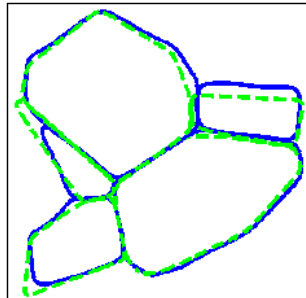
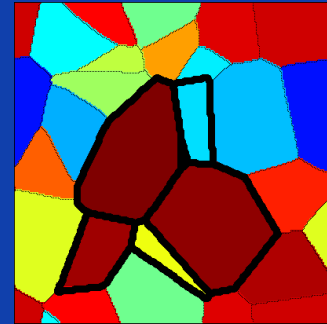
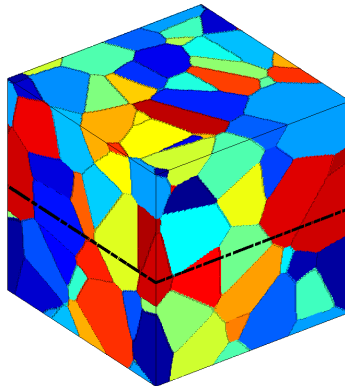


*N. Moelans, F. Wendler, B. Nestler, Comp. Mater. Sci. 46 (2009) p479*

- 2 orientation variants (2D)

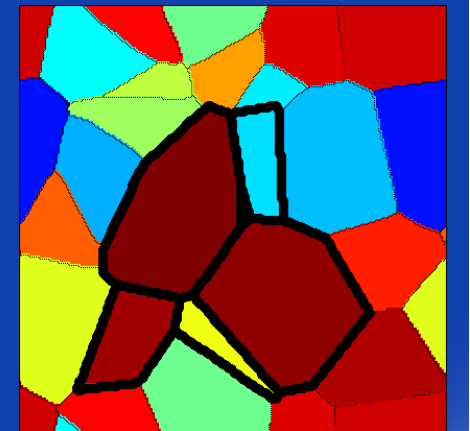
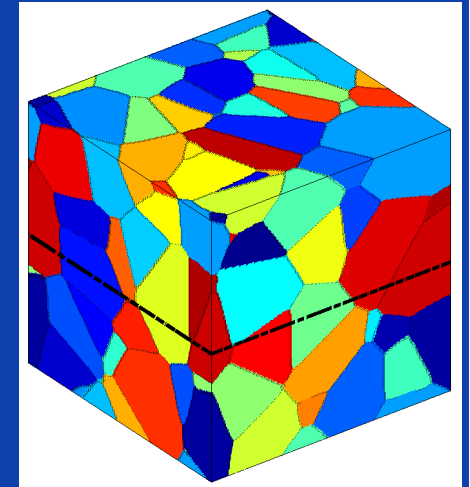
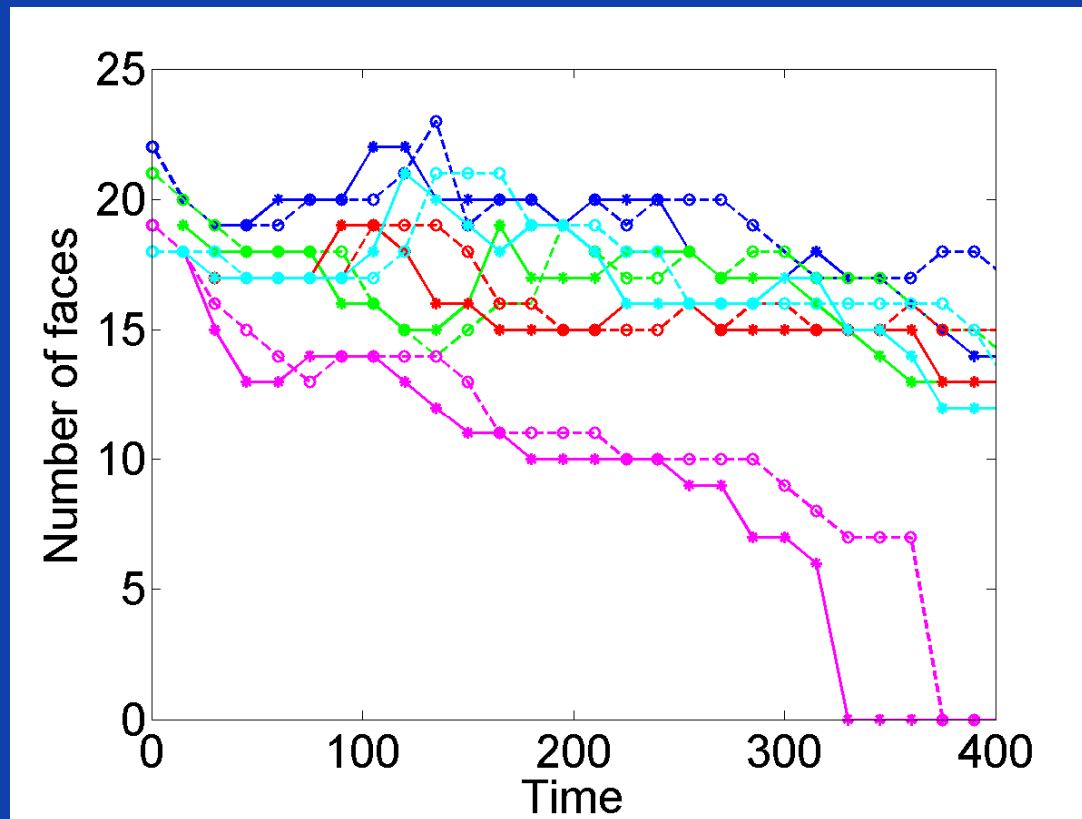


- Isotropic (3D)



N. Moelans, F. Wendler, B. Nestler, *Comp. Mater. Sci.* 46 (2009) p479

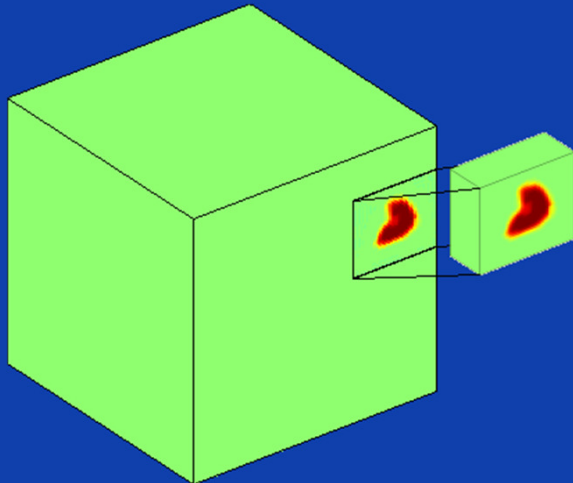
- Isotropic (3D)



*N. Moelans, F. Wendler, B. Nestler, Comp. Mater. Sci. 46 (2009) p479*

- **Basic elements**

- A grain is set of connected grid points  $r$  where  $|\eta_i(r)| > \epsilon$
- For each grain, the corresponding bounding box is the smallest cuboid containing the grain



## Algorithm

- Solve the equations only locally, inside bounding boxes
- Only values inside boxes are kept in memory
- Boxes grow or shrink with grain

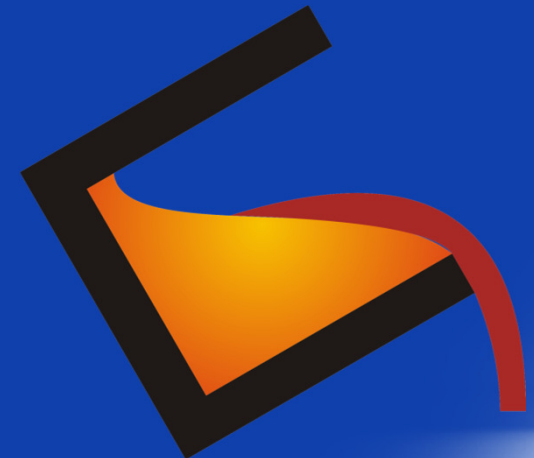
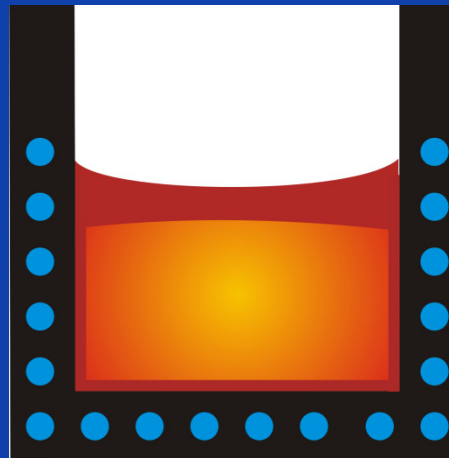
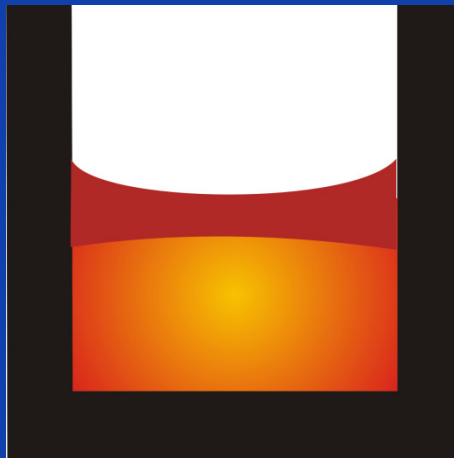
Object Oriented C++ implementation

*Vanherpe et al., PRE, 76, n°056702 (2007)*

## *Application example*

- **Solidification of oxide/silicate melts (slags, lava, magma)**

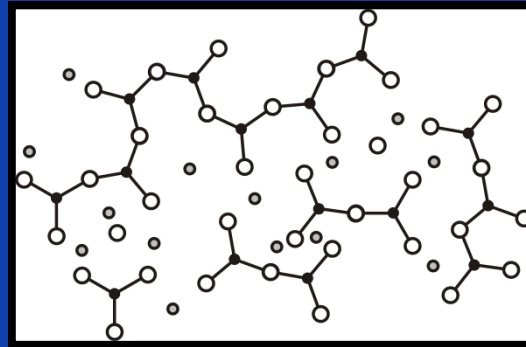
- **Crystallization of slags often occurs in industrial practice**
  1. **Slag in contact with refractory**  
*Solid-liquid interaction between liquid and solid oxide material*
  2. **Freeze lining due to water-cooled furnace**  
*Instantaneously formed layer of crystallized slag*
  3. **Tapping and cooling of slag to ambient temperature**  
*Crystallization of the slag while cooling down*





**Geology**

• **Lava (magma)**



- **Oxide melt**
- $\text{SiO}_2$ ,  $\text{Al}_2\text{O}_3$ ,  $\text{CaO}$ ,  $\text{FeO}$ ,  $\text{Fe}_2\text{O}_3$ ,  $\text{MgO}$  ...
- **High temperature and/or pressure**



**Pyrometallurgy**

• **Slags**

## *Specific to slag solidification*

### Slag solidification

- Mostly facet growth
- Strong anisotropy
- High interfacial energies
- Partial crystallization
- Glass transition
- Oxides are diffusing
- Possible redox reactions

# *Phase field model for slag crystallization*

- Model can treat any number of phases
- Model can treat any number of components
  - CaO, Al<sub>2</sub>O<sub>3</sub>, FeO, Fe<sub>2</sub>O<sub>3</sub>, SiO<sub>2</sub>, ...
- Model is coupled with thermodynamic database (FACT)
- Stoichiometric solid oxide phases
- Diffusion coefficients are taken from the literature, e.g.

$$D^L = \begin{bmatrix} 8.734 & -2,464 \\ -3,948 & 5.977 \end{bmatrix} 10^{-11}$$

- Dendrites and faceted crystals

*J. Heulens et al., Acta Mater. 59 (2011) p2156*

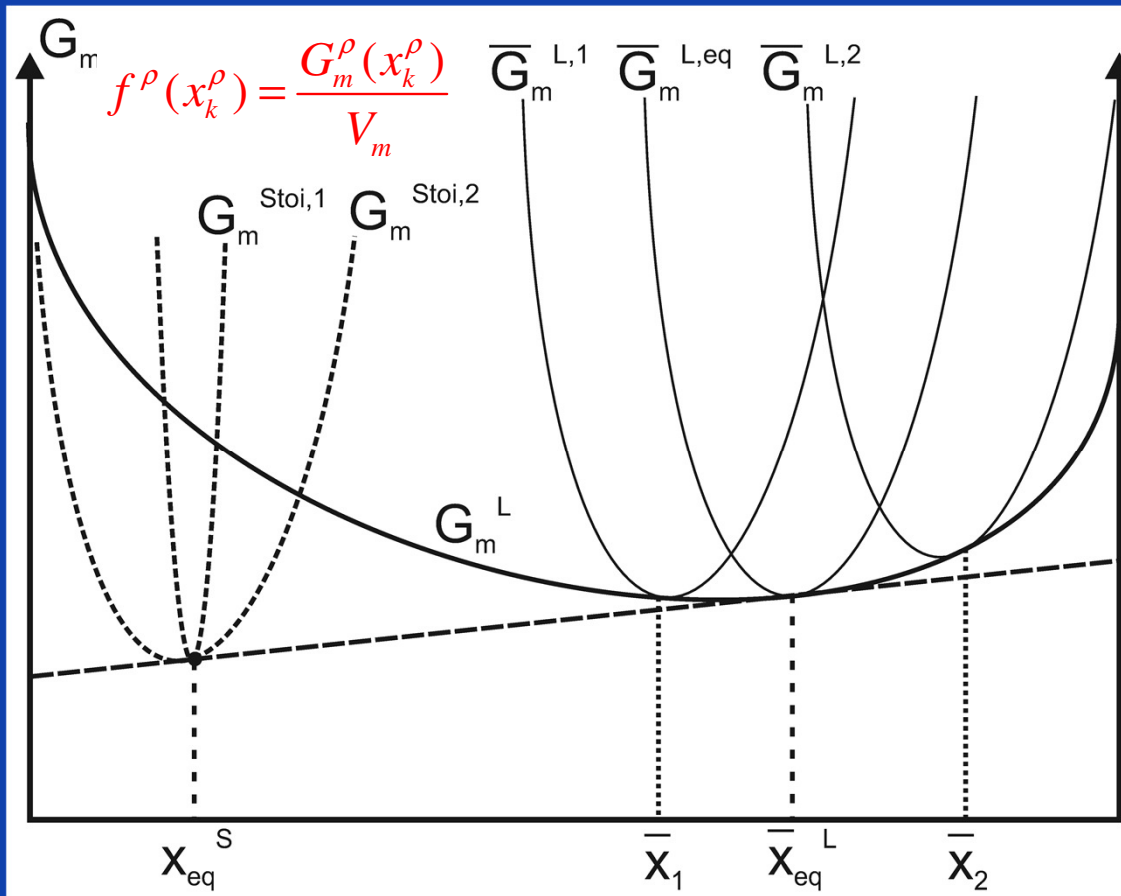
- System of  $p$  phases and  $c$  components
- Phase fields evolve by energy minimization:

$$\frac{\partial \eta_i}{\partial t} = -L(\eta) \frac{\delta}{\delta \eta_i} \left( \int_V \left( mf_0(\eta) + \frac{\kappa(\eta)}{2} \sum_{r=1}^p |\nabla \eta_r|^2 + f_{chem} \right) dV \right)$$

- **Interfacial energy** (Double well and gradient term)
- **Chemical energy** (Gibbs energies of phases)
- Diffusion equation for every component  $k$ :

$$\frac{\partial x_k}{\partial t} = \nabla \cdot \left( \sum_{i=1}^p \phi_i \sum_{r=1}^{c-1} M_{rk}^i \nabla \tilde{\mu}_r^i \right)$$

$$\tilde{\mu}_r^i = \mu_r^i - \mu_{SiO_2}^i$$



- **KKS approach**

$$f_{chem} = \sum_{\rho=1}^p \phi_\rho f^\rho(x_k^\rho)$$

- **Solve  $x_k^\rho$  from**

$$\left\{ \begin{array}{l} \frac{\partial f^\alpha(x_k^\alpha)}{\partial x_k^\alpha} = \frac{\partial f^\beta(x_k^\beta)}{\partial x_k^\beta} \\ \dots = \frac{\partial f^\rho(x_k^\rho)}{\partial x_k^\rho} = \tilde{\mu}_k \\ x_k = \sum_{\rho} \phi_\rho x_k^\rho \end{array} \right.$$

- **At discrete compositions Gibbs energy approximated with parabola**

*J. Heulens et al., Acta Mater. 59 (2011) p2156*

- At discrete  $x_k$  Gibbs energy of phase  $i$  approximated by

$$\hat{f}^i = \sum_{k=1}^{c-1} \left( \frac{A_{kk}^i}{2} (x_k^i - \hat{x}_k^i)^2 + \sum_{l \neq k}^{c-1} A_{kl}^i (x_k^i - \hat{x}_k^i)(x_l^i - \hat{x}_l^i) + B_k^i (x_k^i - \hat{x}_k^i) \right) + C^i$$

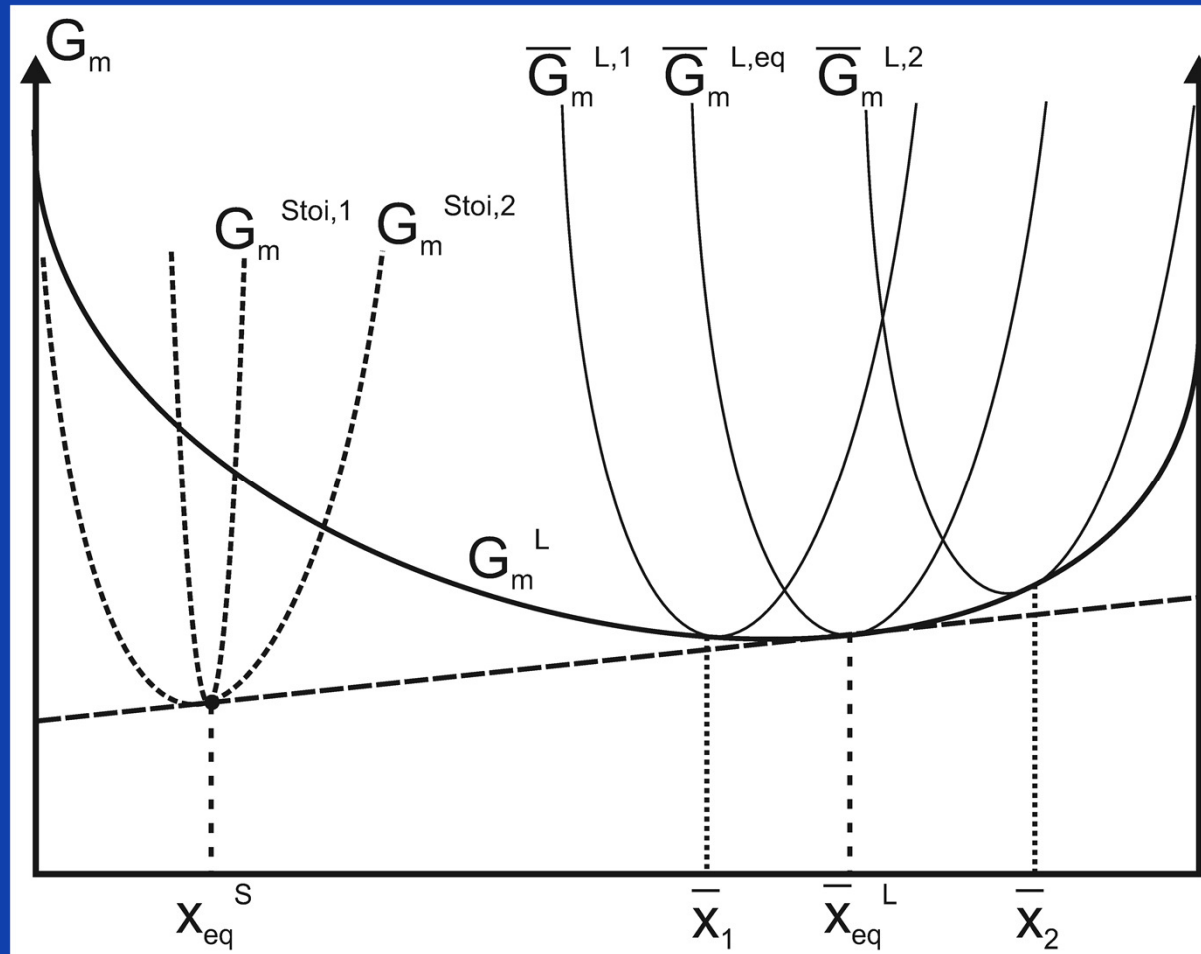
$$A_{kl}^i = \frac{\partial^2 f^i}{\partial x_k^i \partial x_l^i}$$

$$B_k^i = \frac{\partial f^i}{\partial x_k^i} = \tilde{\mu}_k^i$$

$$C^i = f^i$$

- A, B and C are retrieved by ChemApp and stored in an array to load in the phase field code before start simulation
- Diffusion potentials are linear in concentrations, which greatly reduces computational effort

*J. Heulens et al., Acta Mater. 59 (2011) p2156*



- Parabola for Gibbs energy of stoichiometric phase

- Dendrites -- Diffusion controlled
  - Anisotropic energy

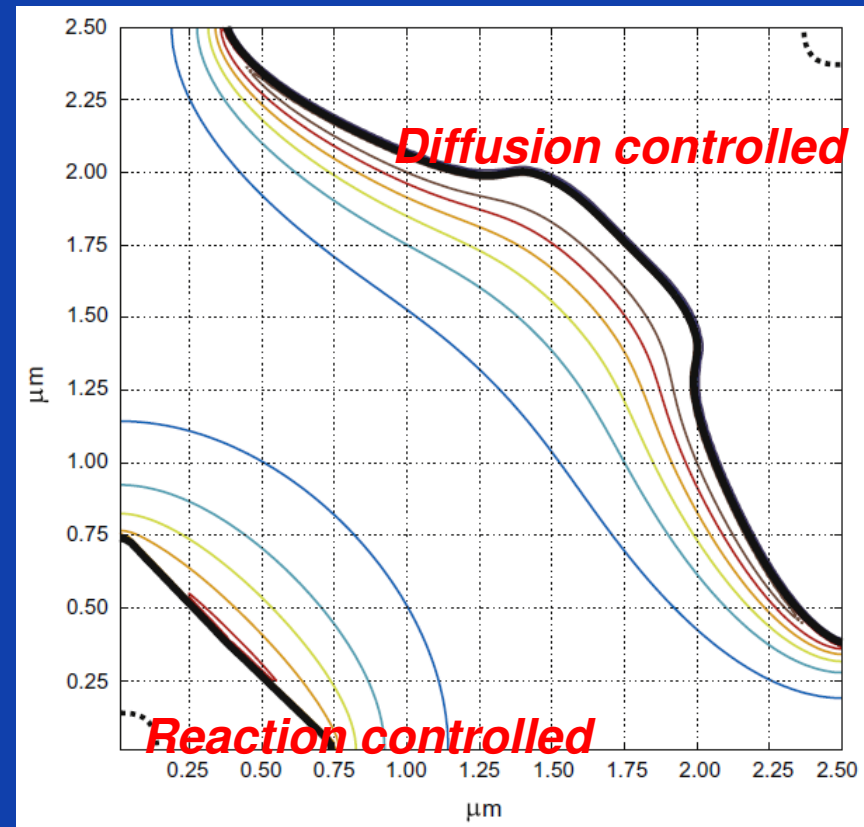
$$\sigma_{i,j} = \bar{\sigma}_{i,j} \left( 1 + \delta_{i,j} \cos(a_{i,j} \theta_{i,j}) \right)$$

- Facets –reaction controlled
  - Anisotropic kinetics

$$L_{i,j} = \bar{L}_{i,j} \left( 1 - \beta_{i,j} + 2\beta_{i,j} \tanh \left( \frac{r_{i,j}}{\left| \tan(0.5a_{i,j}\theta_{i,j}) \right|} \right) \right)$$

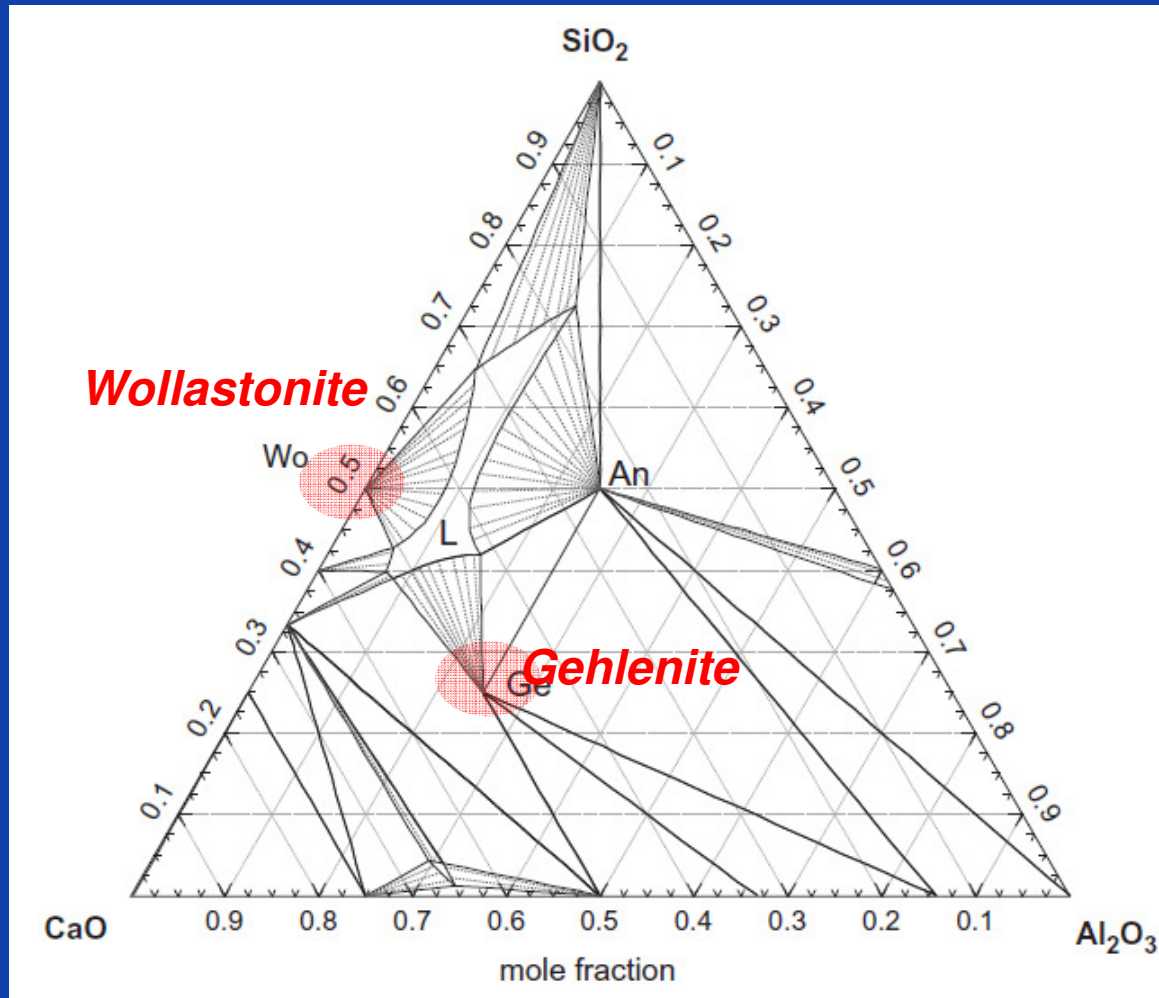
T. Uehara and RF Sekerka, *J. Cryst. Growth* (2003) 254, p251.

J. Heulens et al., *Acta Mater.* 59 (2011) p2156

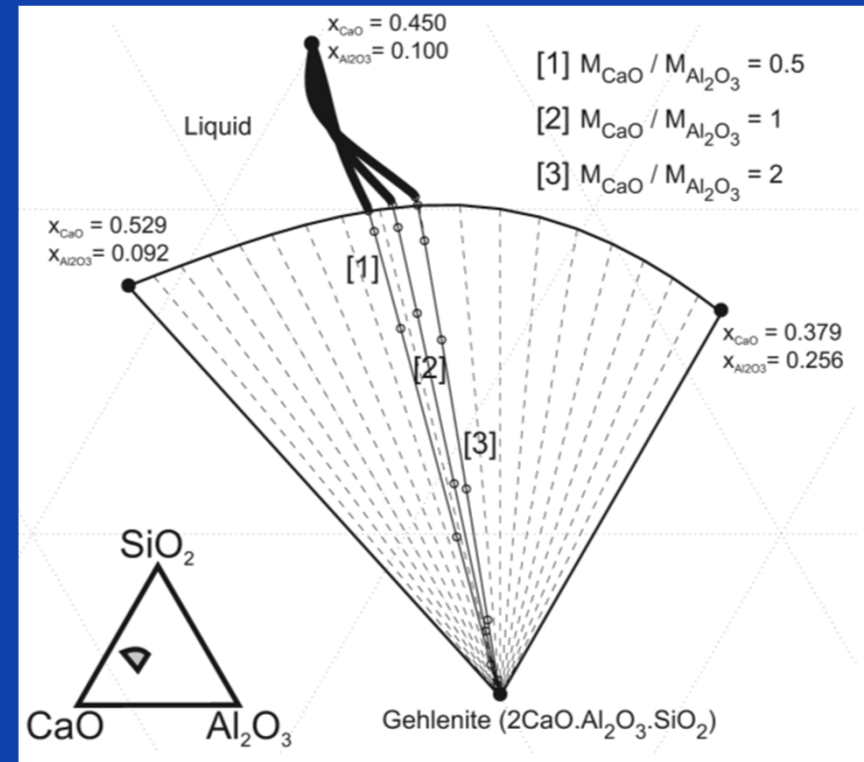
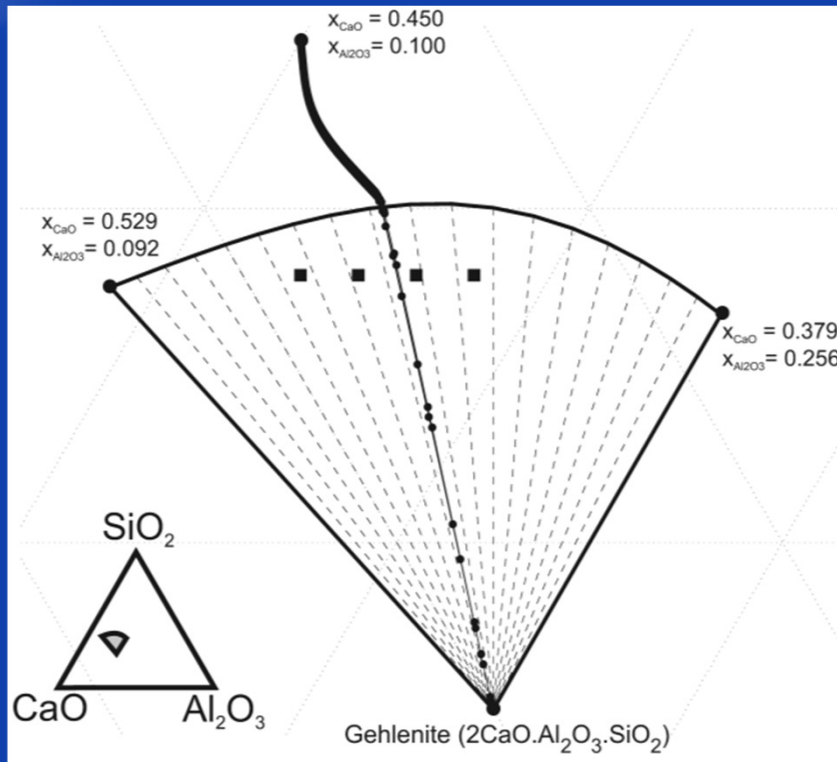


Interface orientation

$$\theta_{i,j} = \arctan \left| \frac{\nabla_y \eta_i - \nabla_y \eta_j}{\nabla_x \eta_i - \nabla_x \eta_j} \right|$$



# Dissolution of Gehlenite

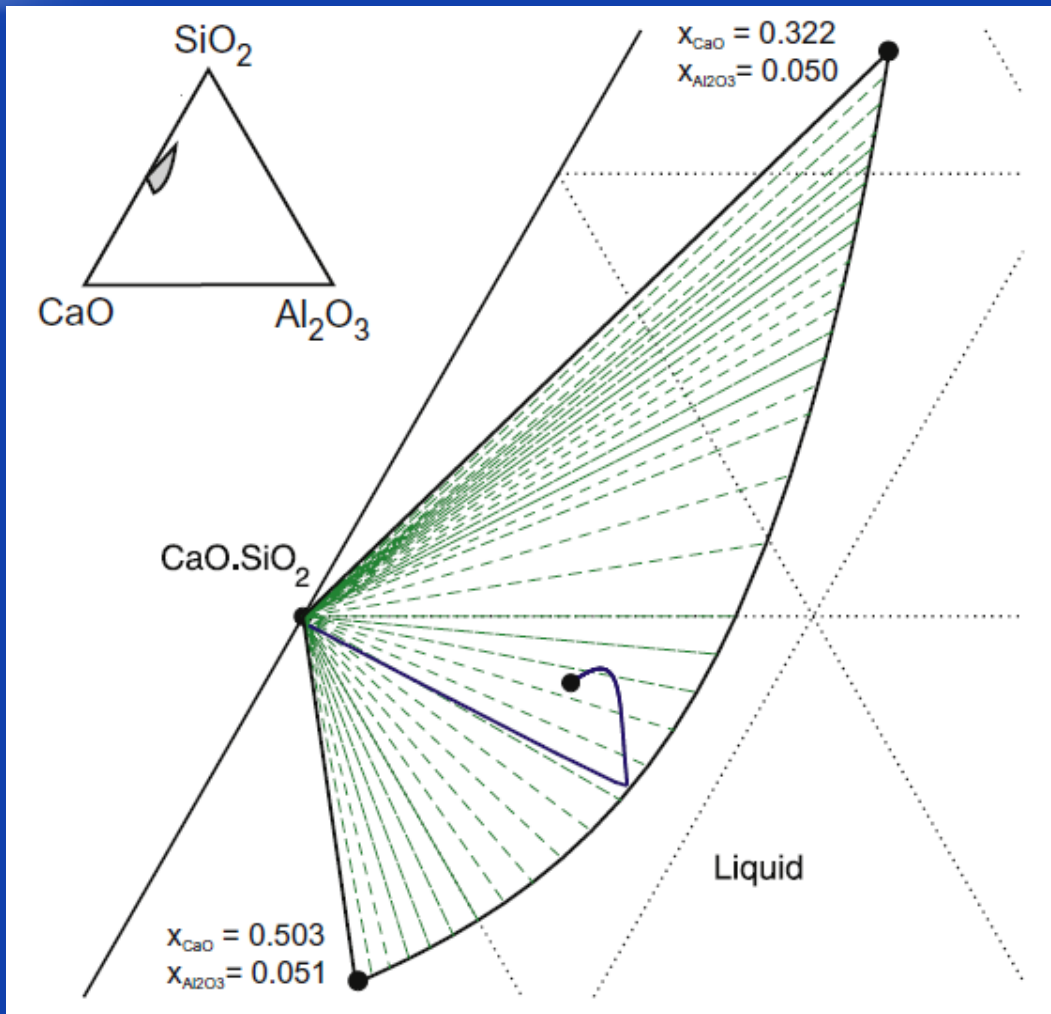


*Parabola construction with minimal influence on results*

*Tie-line selection depending on diffusion kinetics in liquid*

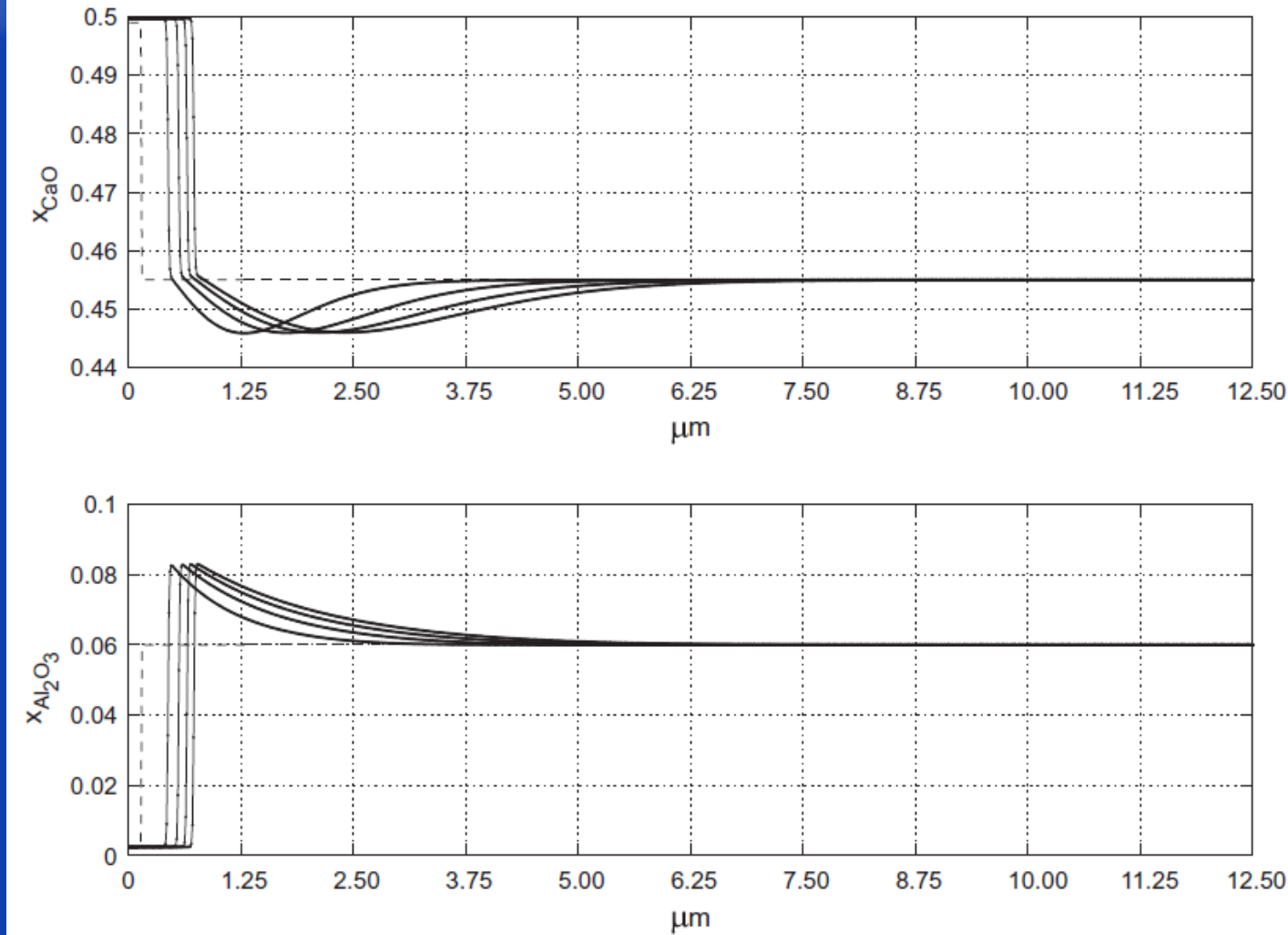
J. Heulens et al., Acta Mater. 59 (2011) p2156

# Crystallization Wollastonite (1D)



- Uphill diffusion
- Automatic tie-line selection

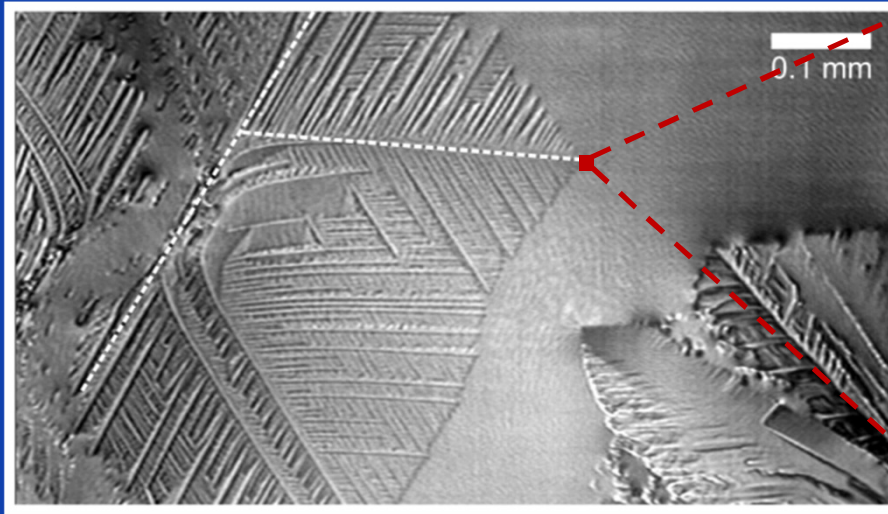
# Crystallization Wollastonite (1D)



- Uphill diffusion
- Automatic tie-line selection

# Crystallization Wollastonite (2D)

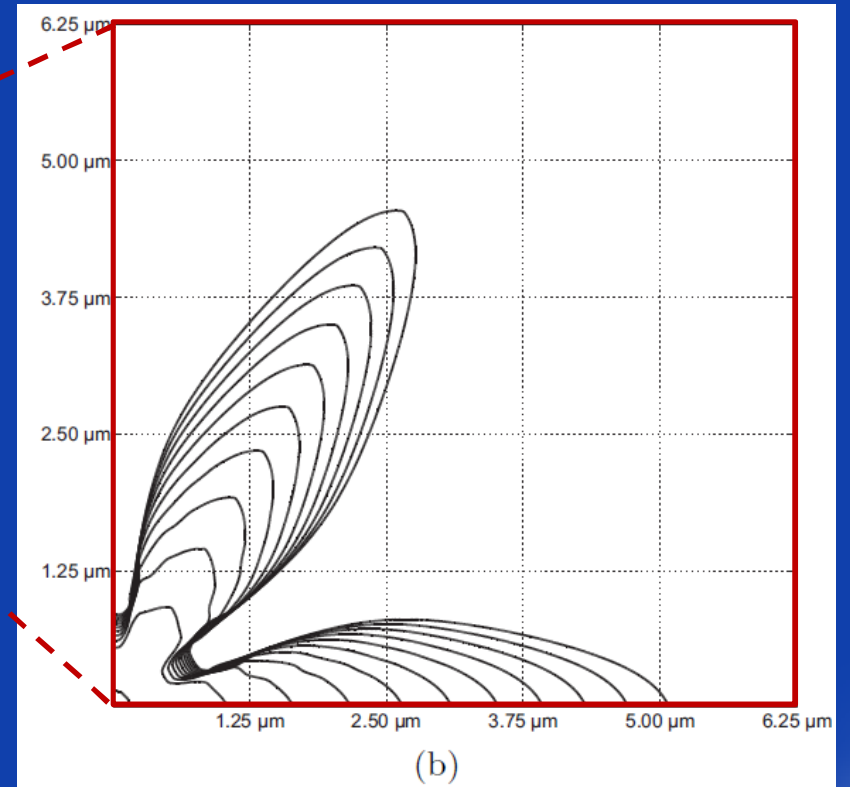
*Experiment*



*Growth of wollastonite in  $42\text{CaO}-10\text{Al}_2\text{O}_3-48\text{SiO}_2$  at  $1320^\circ\text{C}$*

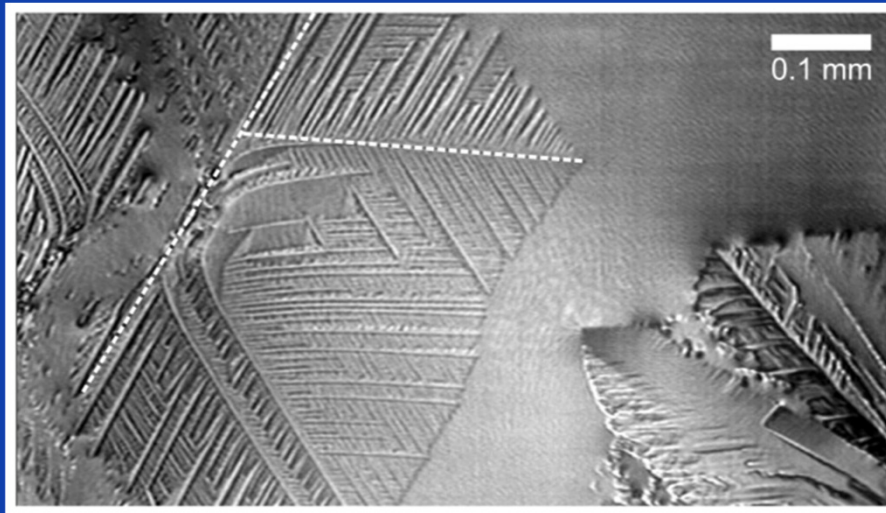
*Confocal laser microscope*

*Simulation*



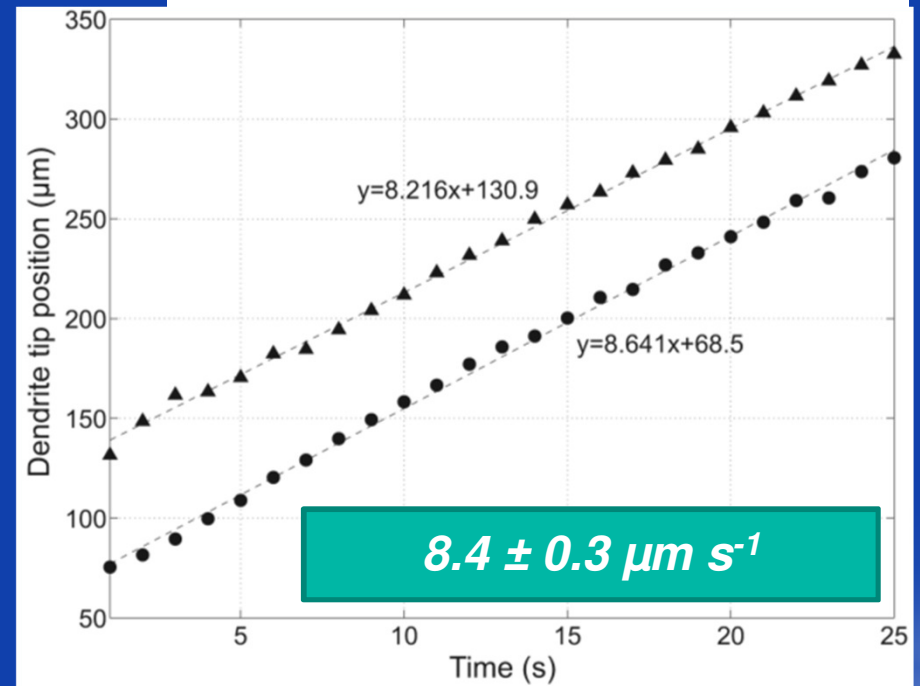
*Computer cluster (100 cpu)*

- Confocal Laser Scanning Microscope (CLSM)
- At low undercooling (1370°C) → faceted growth
- At high undercooling (1320°C) → dendrite growth with 6-fold anisotropy



*Hexagonal dendrites of  $\text{CaSiO}_3$  in  $\text{CaO-Al}_2\text{O}_3\text{-SiO}_2$  @1320°C*

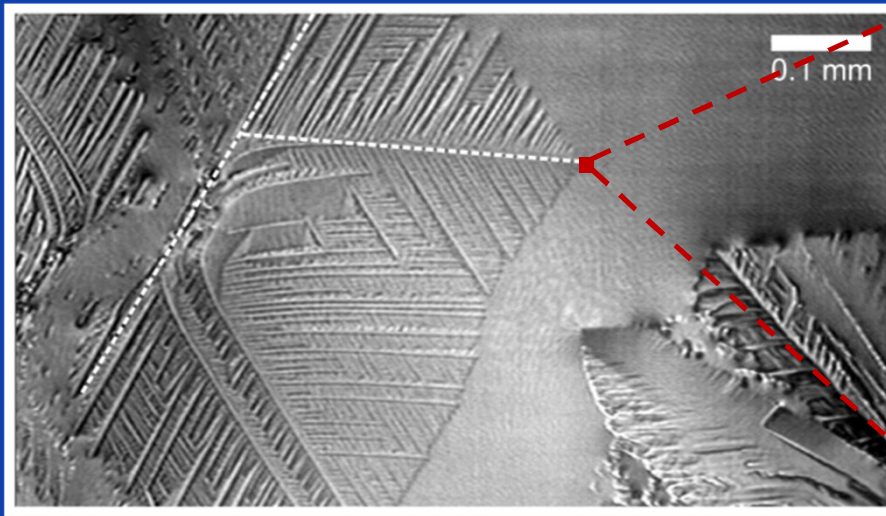
**Linear growth at steady-state**



*J. Heulens et al., J. Eur. Cer. Soc. 31 (2011) p1873*

# Crystallization Wollastonite (2D)

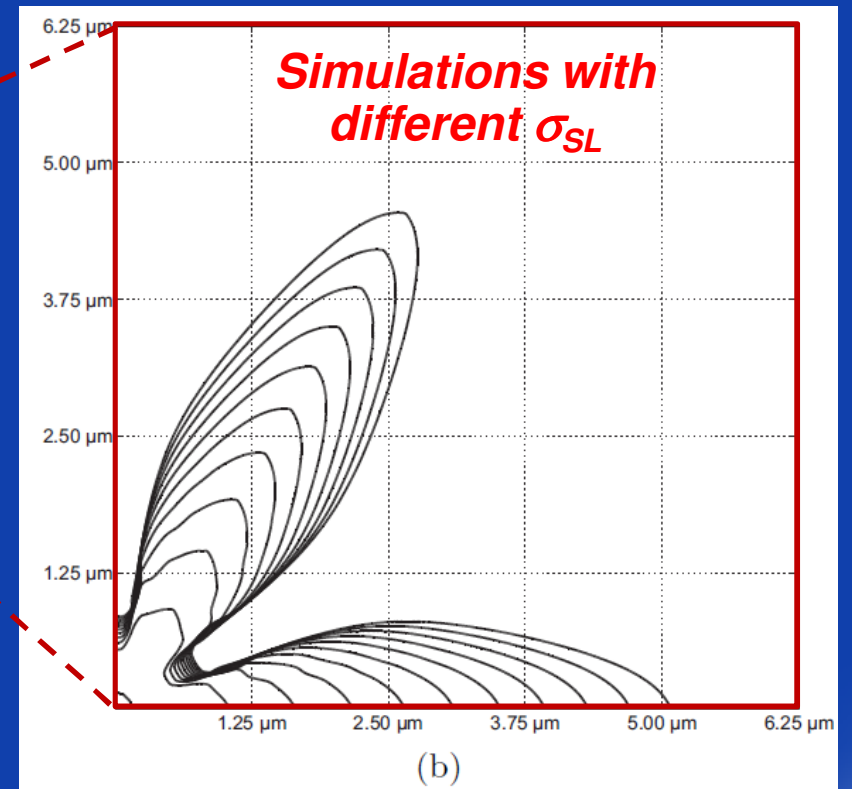
**Experiment**



**Growth of wollastonite in  $42\text{CaO}-10\text{Al}_2\text{O}_3-48\text{SiO}_2$  at  $1320^\circ\text{C}$**

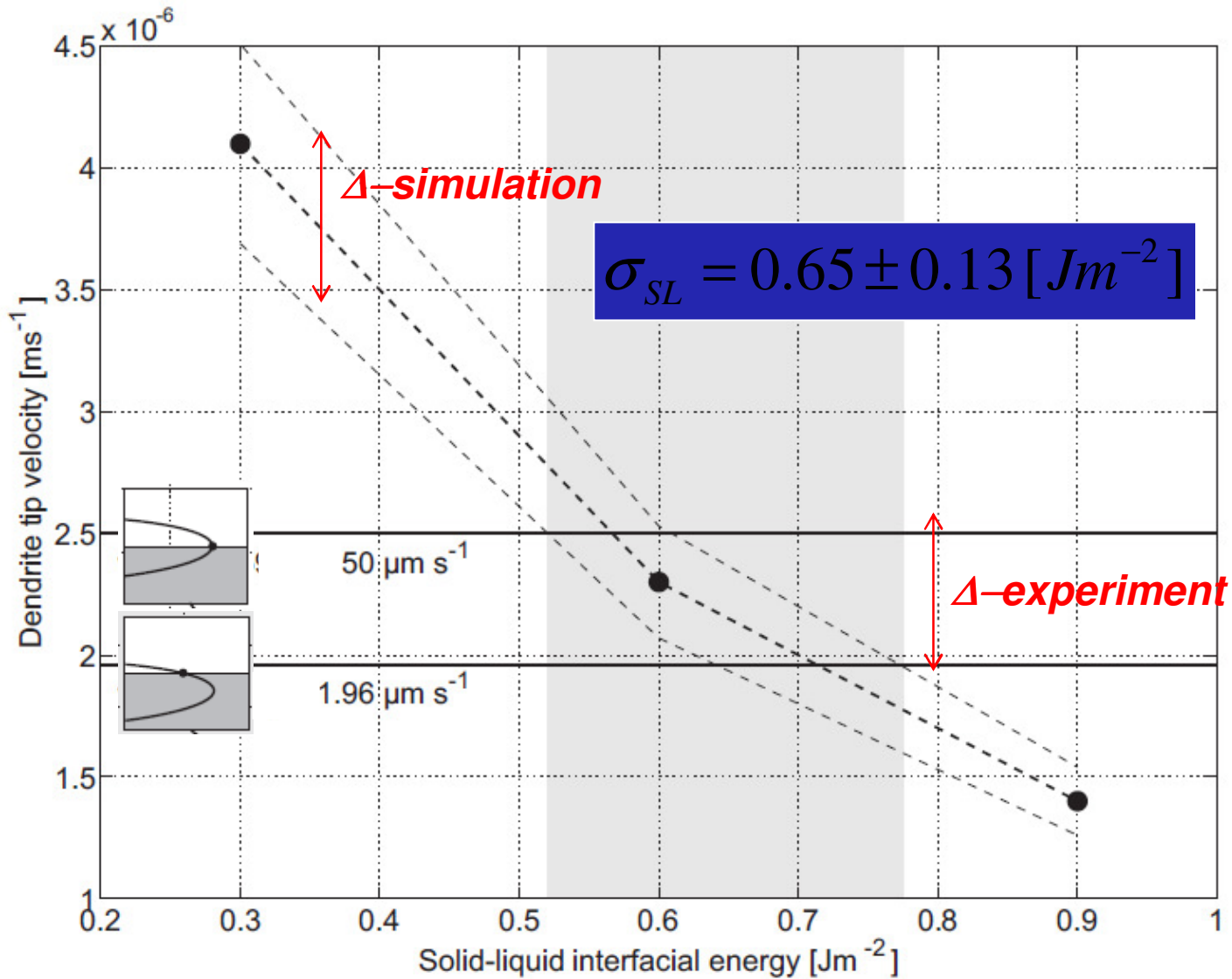
**Confocal laser microscope**

**Simulation**



**Computer cluster (100 cpu)**

# Estimation of the S-L interfacial energy



# *Oxidation state dependent crystallization*

- System :  $\text{FeO-Fe}_2\text{O}_3\text{-SiO}_2$  @  $1400^\circ\text{C}$ 
  - Crystallization of magnetite ( $\text{FeO}\cdot\text{Fe}_2\text{O}_3$ )
  - Local oxidation state in liquid
  - Open system in contact with  $\text{O}_2$  atmosphere (fixed  $p_{\text{O}_2}$ )



*J. Heulens et al., Chem. Geology, 290 (2011) p156*

# *Oxidation state dependent crystallization*

- System : FeO-Fe<sub>2</sub>O<sub>3</sub>-SiO<sub>2</sub> @ 1400°C
  - Crystallization of magnetite (FeO·Fe<sub>2</sub>O<sub>3</sub>)
  - Local oxidation state in liquid
  - Open system in contact with O<sub>2</sub> atmosphere (fixed  $p_{O_2}$ )
- Redox reactions
  - Redox reactions in local equilibrium
  - Fe<sup>3+</sup> / Fe<sup>2+</sup> direct measure for local oxygen potential (true within limited composition and  $p_{O_2}$  range)
  - O<sub>2</sub> diffusion by changing the Fe<sup>3+</sup> / Fe<sup>2+</sup> ratio -> diffusion of FeO and Fe<sub>2</sub>O<sub>3</sub> is considered



# Oxidation state dependent crystallization

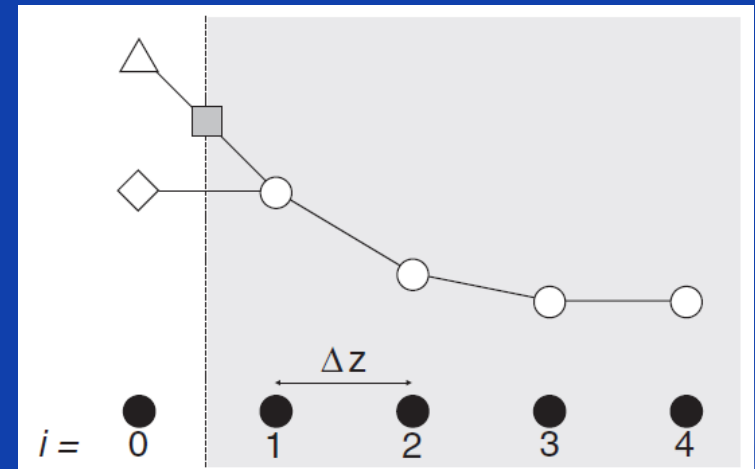
- System : FeO-Fe<sub>2</sub>O<sub>3</sub>-SiO<sub>2</sub> @ 1400°C
  - Crystallization of magnetite (FeO·Fe<sub>2</sub>O<sub>3</sub>)
  - Local oxidation state in liquid
- Open system in contact with O<sub>2</sub> atmosphere (fixed  $p_{O_2}$ )
  - Special boundary condition to preserve Fe but not O
    - Mass balance Fe



$$x_{FeO}^{i=0} + 2x_{Fe_2O_3}^{i=0} = x_{FeO}^{i=1} + 2x_{Fe_2O_3}^{i=1}$$

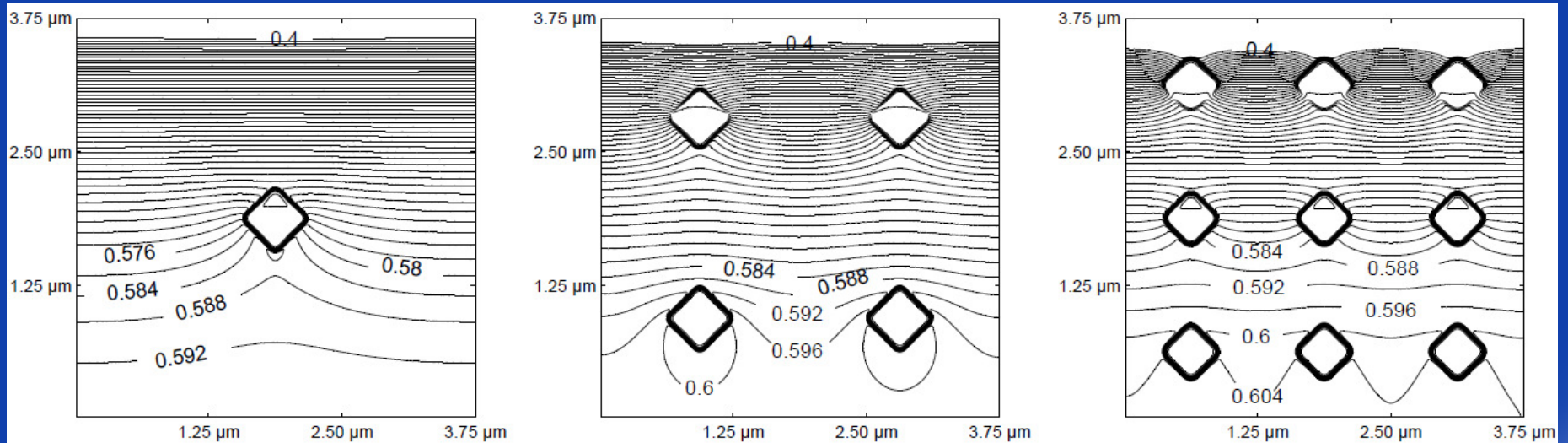
– Fixed  $p_{O_2}$

$$\frac{x_{FeO}^{i=0.5}}{x_{Fe_2O_3}^{i=0.5}} = cte(p_{O_2,atm})$$



*J. Heulens et al., Chem. Geology, 290 (2011) p156*

- Atmosphere:  $p_{O_2}=1.5 \times 10^{-3}$  ; Initial melt:  $a_{O_2}= 2.4 \times 10^{-5}$ 
  - Oxidation from atmosphere
  - Reduction from growth of  $Fe_3O_4$
- Faceted reaction controlled growth

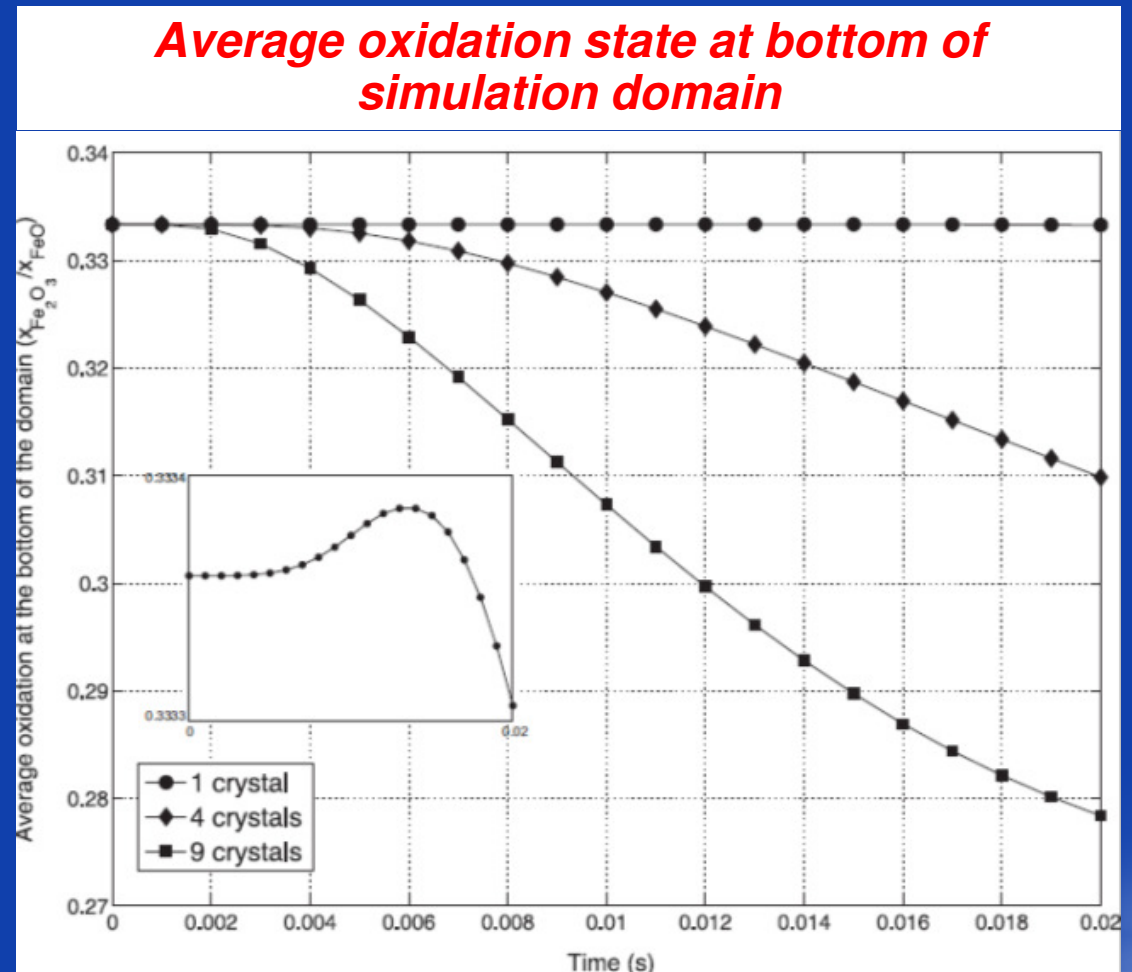


**Contour plots  $x_{FeO}$**

*J. Heulens et al., Chem. Geology, 290 (2011) p156*

# Crystallization of magnetite

- Melt is reduced
  - Faster for higher crystal density
  - Some oxidation initially for low crystal density
- Limited effect of  $p_{O_2}$  atmosphere on  $a_{O_2}$  melt due to crystallization
  - e.g. rhyolite lavas in Yellowstone Park
- $p_{O_2}$  atmosphere affects crystal growth



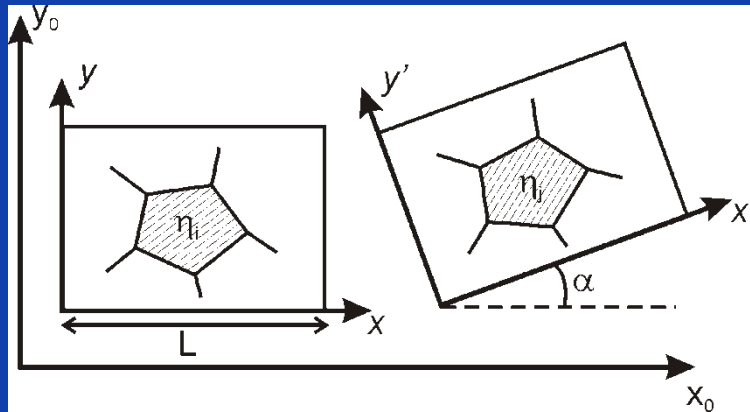
- What do we need further to improve the quantitative accuracy for polycrystalline and multi-phase systems ?
  - Accurate representation of triple-junction angles outside  $[100^\circ - 140^\circ]$   $\leftrightarrow$  equal interface width
  - General solution for chemical potential jump accros interface
  - (CALPHAD) Gibbs/free energies over full composition domain (stoichiometric phases, metastable regions)
  - Composition and orientation dependent expressions for diffusion and interfacial properties
  - Elastic and plastic effects

- OT/07/040 (Quantitative phase field modelling of coarsening in lead-free solder joints)
- IUAP Program DISCO (Dynamical Systems, Control, and Optimization)
- IWT grant SB-73163 (Phase-Field Modelling of the Solidification of Oxidic Systems)
- Research Foundation - Flanders (FWO-Vlaanderen)
- Simulations were performed on the Flemisch Super Computer (VSC)
  
- More information on <http://nele.studentenweb.org> and <https://www.mtm.kuleuven.be/Onderzoek/Semper/SolMicS/>

- Thank you for your attention !! Questions ?

# Rotation invariance of the model

- Mathematically, the model equations are invariant to rotation, but ...
- the order parameters represent orientations in a fixed reference frame.



grid spacing  $\Delta h$

physical width of domain  $L$

rotational symmetry  $n$

- The precision of  $\alpha$  depends on the numerical setup,

$$\Delta\alpha \approx \frac{1}{\cos\alpha} \frac{\Delta h}{L}$$

- For the model to be rotational invariant in practice, lower limit of amount of order parameters  $p$ :

$$p > \frac{\sqrt{2}\pi L}{n\Delta h}$$

*J. Heulens and N. Moelans, Scripta Mat. (2010)*

## Principles of the matched asymptotic expansion

Expansion inner region:

$$\eta(n/\varepsilon, t_1, t_2) = \eta_0(n/\varepsilon, t_1, t_2) + \varepsilon \eta_1(n/\varepsilon, t_1, t_2) + \dots$$

$$c(n/\varepsilon, t_1, t_2) = c_0(n/\varepsilon, t_1, t_2) + \varepsilon c_1(n/\varepsilon, t_1, t_2) + \dots$$

Expansion outer regions:

$$\eta^*(n, t_1, t_2) = \eta_0^*(n, t_1, t_2) + \varepsilon \eta_1^*(n, t_1, t_2) + \dots$$

$$c^*(n, t_1, t_2) = c_0^*(n, t_1, t_2) + \varepsilon c_1^*(n, t_1, t_2) + \dots$$

Match inner and outer region:

$$\lim_{n/\varepsilon \rightarrow \pm\infty} \eta_0(n/\varepsilon) = [\eta_0^*]^\pm, \quad \lim_{n/\varepsilon \rightarrow \pm\infty} \eta_j(n/\varepsilon) = \dots$$

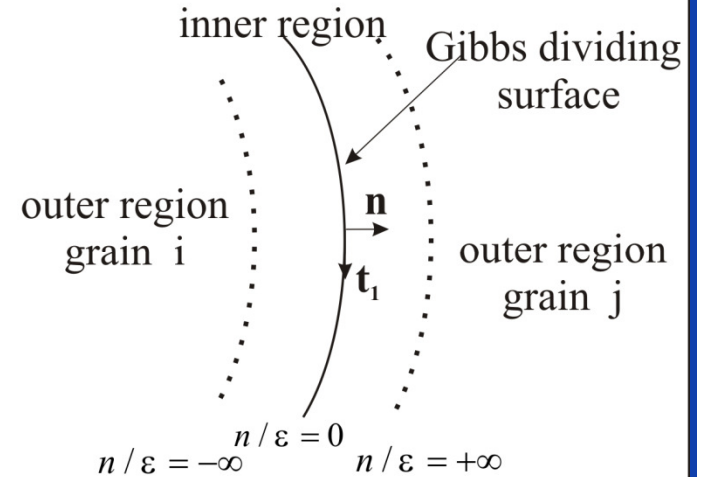
$$\lim_{n/\varepsilon \rightarrow \pm\infty} c_0(n/\varepsilon) = [c_0^*(0)]^\pm, \quad \lim_{n/\varepsilon \rightarrow \pm\infty} c_j(n/\varepsilon) = \dots$$

gives sharp-interface model with corrections

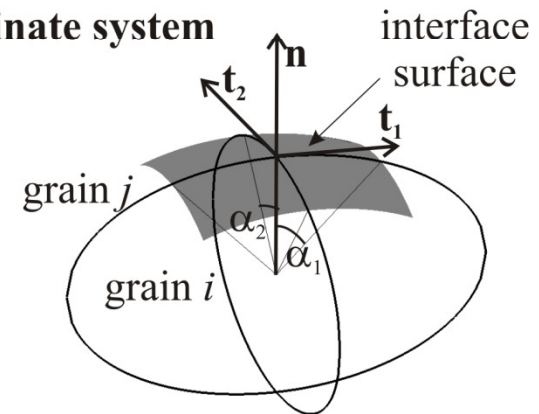
Gibbs Thomson  $\frac{c_\alpha^i}{c_\alpha^{eq}} = 1 - (1-k)d_0K - (1-k)\beta v_n + corr(O(\varepsilon^v))$

with  $k = \frac{c_\beta^i}{c_\alpha^i}$

Conservation  $(c_\alpha^i - c_\beta^i)v_n = [D\partial_n c]_+ + corr(O(\varepsilon^v))$



3D curvilinear coordinate system



- **Multi-phase-field model**

- **Phase fields**  $\phi_1, \phi_2, \phi_3, \dots, \phi_p$ ,  $\sum_{i=1}^p \phi_i = 1$

- **Interfacial energy**  $f_{\text{int}} = \sum_{i \neq j} \frac{4\sigma_{i,j}}{\eta_{i,j}} \left\{ \frac{\eta_{i,j}^2}{\pi^2} |\nabla \phi_i \cdot \nabla \phi_j| + \phi_i \phi_j \right\}$   
 $0 < \phi_{i,j} < 1$

*Steinbach et al.*

*MICRESS phase-field code*

H. Garcke, B. Nestler,  
B. Stoth, SIAM J. Appl.  
Math. 60 (1999) p 295.

- Multi-phase-field model

- Multi-order parameter models

$$\eta_1, \eta_2, \dots, \eta_i(r, t), \dots, \eta_p, \quad \left( \sum_{i=1}^p \eta_i \neq 1 \right)$$

L.-Q. Chen and W. Yang,  
PRB, 50 (1994) p15752

- Order parameters

$$f_{\text{int}} = m \left( \sum_{i=1}^p \left( \frac{\eta_i^4}{4} - \frac{\eta_i^2}{2} \right) + \sum_{i=1}^p \sum_{j<i}^p \gamma_{i,j} \eta_i^2 \eta_j^2 + \frac{1}{4} \right) + \frac{\kappa(\eta)}{2} \sum_{i=1}^p (\vec{\nabla} \eta_i)^2$$

- Interfacial energy

$$\kappa(\eta) = \frac{\sum_{i=1}^p \sum_{j<i}^p \kappa_{i,j} \eta_i^2 \eta_j^2}{\sum_{i=1}^p \sum_{j<i}^p \eta_i^2 \eta_j^2}$$

A. Kazaryan et al., PRB,  
61 (2000) p14275

- **Multi-phase-field model**

- **Phase fields**  $\phi_1, \phi_2, \phi_3, \dots, \phi_p$ ,  $\sum_{i=1}^p \phi_i = 1$

- **Interfacial energy**  $f_{\text{int}} = \sum_{i \neq j} \frac{4\sigma_{i,j}}{\eta_{i,j}} \left\{ \frac{\eta_{i,j}^2}{\pi^2} |\nabla \phi_i \cdot \nabla \phi_j| + \phi_i \phi_j \right\}$   
 $0 < \phi_{i,j} < 1$

*Steinbach et al.*

*MICRESS phase-field code*

H. Garcke, B. Nestler,  
B. Stoth, SIAM J. Appl.  
Math. 60 (1999) p 295.

- **Multi-order parameter models**

- **Order parameters**  $\eta_1, \eta_2, \dots, \eta_i(\vec{r}, t), \dots, \eta_p$ ,  $\left( \sum_{i=1}^p \eta_i \neq 1 \right)$

- **Interfacial energy**  $f_{\text{int}} = m \left( \sum_{i=1}^p \left( \frac{\eta_i^4}{4} - \frac{\eta_i^2}{2} \right) + \sum_{i=1}^p \sum_{j < i}^p \gamma_{i,j} \eta_i^2 \eta_j^2 + \frac{1}{4} \right) + \frac{\kappa(\eta)}{2} \sum_{i=1}^p (\nabla \eta_i)^2$

$$\kappa(\eta) = \frac{\sum_{i=1}^p \sum_{j < i}^p \kappa_{i,j} \eta_i^2 \eta_j^2}{\sum_{i=1}^p \sum_{j < i}^p \eta_i^2 \eta_j^2}$$

*L.-Q. Chen and W. Yang,*  
*PRB, 50 (1994) p15752*

*A. Kazaryan et al., PRB,*  
*61 (2000) p14275*

- **Vector valued model**

- **Orientation field ( $\theta$ ) and phase field ( $\phi$ )**

- **Free energy**  $f_{\text{int}} = f(\phi, |\nabla\phi|, |\nabla\theta|)$

*R. Kobayashi, J.A. Warren,  
W.C. Carter, Physica D, 119  
(1998) p415*

- **2-phase solidification**

- **Phase fields**  $\phi_1, \phi_2, \phi_3, \sum_{i=1}^3 \phi_i = 1$

- **Free energy**  $f_{\text{int}} = f(\phi_1, \phi_2, \phi_3) + \frac{\kappa}{2} \sum_{i=1}^3 (\nabla\phi_i)^2$

*R. Folch and M. Plapp, PRE, 72  
(2005) n° 011602*

- **No third-phase contributions**
- **Bulk energy interpolation function with 0-slope**